Seismic Design of Unbonded Post-Tensioned Precast Concrete Walls with Vertical Joint Connectors

Felipe J. Perez
Ph.D. Candidate
Department of Civil and Environmental Engineering
Lehigh University
Bethlehem, Pennsylvania

Stephen Pessiki, Ph.D.
Associate Professor of Structural Engineering
Department of Civil and Environmental Engineering
Lehigh University
Bethlehem, Pennsylvania

Richard Sause, Ph.D.
Professor of Structural Engineering
Director, ATLSS Research Center
Lehigh University
Bethlehem, Pennsylvania

This paper presents an investigation of the seismic design of precast concrete wall panels connected along vertical joints with ductile connectors and to the foundation along horizontal joints using unbonded post-tensioning steel. Closed-form expressions are derived to estimate key values defining a trilinear idealized lateral load behavior of the walls. A proposed seismic design approach is developed using base shear demands recommended by current building codes. Unbonded post-tensioned precast concrete walls with substantial initial lateral stiffness can be designed to resist seismic forces – without yielding of the post-tensioning steel – by absorbing and dissipating energy in the vertical joint connections. In a companion paper ("Lateral Load Behavior of Unbonded Post-Tensioned Precast Concrete Walls with Vertical Joints" scheduled for publication in the next issue of the PCI JOURNAL),[1] the authors describe a fiber-based analytical model used in a design parameter study of several unbonded post-tensioned precast concrete walls with vertical joints. The companion paper presents the results of the analytical parameter study and uses those results to verify the accuracy of the closed-form expressions derived in this paper.

The aftermath of past earthquakes has demonstrated the superior seismic performance of buildings with reinforced concrete walls as the primary lateral load resisting system.[2] Precast concrete construction in particular offers the benefits of quality control, fast erection, cost effectiveness, and construction efficiencies. Use of precast

concrete structural walls for earthquake resistance in buildings combines the benefits of loadbearing walls and precast concrete systems.

The objectives of this study are (1) to derive closed-form expressions for the base-shear-roof-displacement capacities of unbonded post-tensioned precast concrete walls with vertical joint connectors, and (2) to propose a design approach that relates wall capacities to code-specified design demands. Fig. 1 shows an elevation view of the prototype precast concrete wall considered in this investigation. The wall is composed of three two-story, full-height precast concrete panels. Study results also apply to walls with different numbers of panels and different panel sizes.

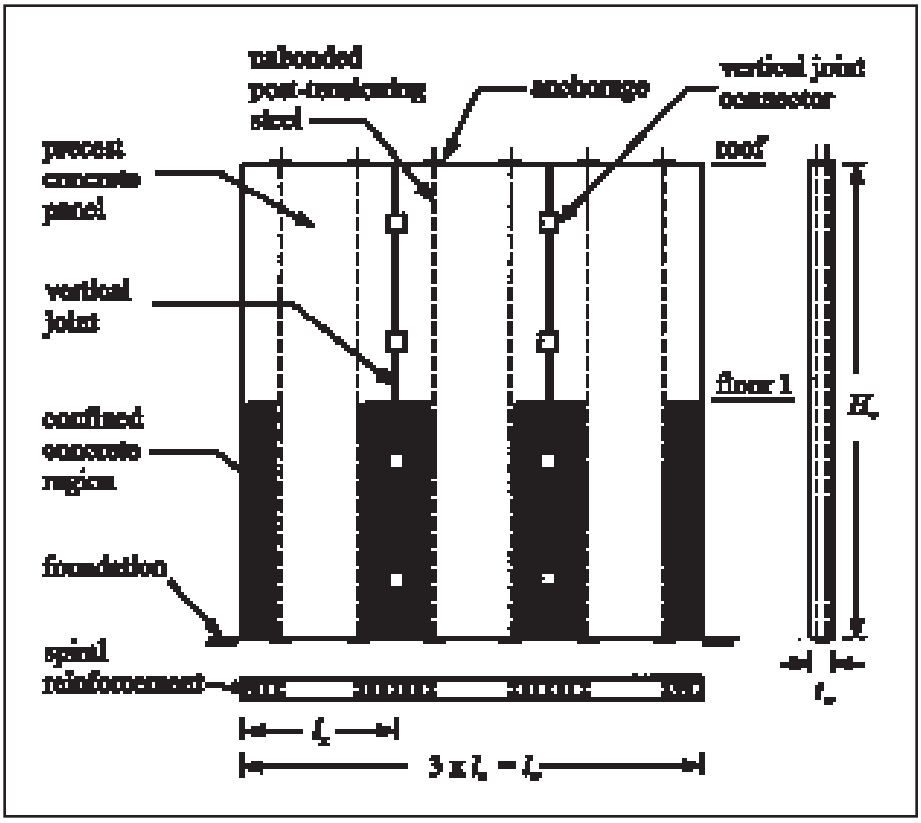

Fig. 1. Precast wall with vertical joints between panels and vertical joint connectors.

Panels are attached to each other along vertical joints with ductile connectors, referred to as vertical joint connectors. The wall panels are attached to the foundation across horizontal joints using unbonded post-tensioning steel (dashed line in Fig. 1) that is anchored at the top of each panel and within the foundation. Confining reinforcement is used to encase the concrete at the ends of each panel throughout the height of the first story. The confining reinforcement shown in Fig. 1 consists of interlocking steel spirals, but other confining details can be used, including hoop reinforcement. Steel confinement enables the bottom concrete in the panels to sustain the large compressive strains that may develop as a result of gap opening displacements along the base of each panel due to lateral loads.

Unbonded post-tensioning is used across the horizontal joints of the wall; compared to bonded post-tensioning steel, unbonded steel yields at a larger overall member deformation.[3] The result is a wall that can undergo large nonlinear lateral displacements without yielding the post-tensioning steel and without a significant loss in self-centering capability.

Vertical joint connectors consist of steel components which are intended to provide vertical shear force transfer between the wall panels and provide energy dissipation under seismic loading. Various vertical joint connection details for precast concrete shear walls have been investigated.[4] In this study, the vertical joint connectors are intended to transfer shear between the wall panels and also to dissipate energy under seismic loading by yielding in shear. Therefore, the prototype wall shown in Fig. 1 has unbonded post-tensioning across horizontal joints, ductile connectors along vertical joints, and confining reinforcement in the panel compression zones. The prototype is expected to sustain large nonlinear lateral displacements by dissipating energy in the vertical joint connectors, without yielding of the post-tensioning steel, significant loss in self-centering capability, or concrete compression failure in the wall panels.

This expected behavior was validated by tests of a 0.6-scale five-story precast concrete building, tested under simulated seismic loading at the University of California, San Diego (UCSD). The building relied on a vertically jointed unbonded post-tensioned precast concrete wall for seismic resistance in one direction of the building, and precast frames in the orthogonal direction.[5] Preliminary results[6] revealed that the wall suffered only minor spalling at the base when the building was tested (in the direction of the wall) at an earthquake intensity of 50 percent higher than the design level ground motion. In addition, the vertical joint connectors provided considerable energy dissipation. Lastly, due to the unbonded post-tensioning, the residual drift was very low after the design level ground motion was applied. Results demonstrate that unbonded post-tensioned precast concrete walls with vertical joint connectors are well suited for use as seismic resistance of building structures.

Design guidelines for unbonded post-tensioned precast walls with vertical joint connectors were published by Stanton and Nakaki.[7] The present study differs from these guidelines in two ways. First, the walls considered by Stanton and Nakaki had unbonded post-tensioning steel and the gravity loads were located at the center of each wall panel. The present study considers two groups of post-tensioning steel that are not necessarily located at the center of each wall panel. In addition, the groups of post-tensioning steel in each panel

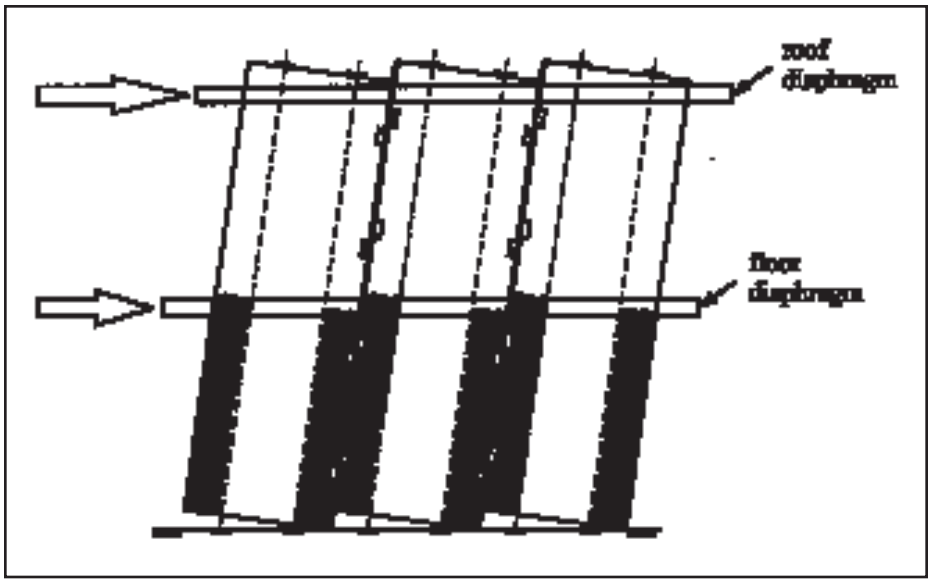

Fig. 2. Lateral load deflected shape of a precast wall with vertical joint connectors.

can have different initial prestress forces, as discussed later. Furthermore, the gravity loads carried by each panel can vary in magnitude along the height of the wall and have a constant eccentricity within each panel that can vary from panel to panel. Therefore, the walls treated by Stanton and Nakaki are a special case of the more generalized walls considered herein.

Second, Stanton and Nakaki considered one limit state in their design approach, corresponding to the onset of yielding of the post-tensioning steel. This study considers additional limit states in the design, some of which are useful in establishing the envelope lateral load response of the walls, and others which are required to ensure overall satisfactory seismic performance of the walls. An unabridged discussion of the material presented here and in the companion paper[1] can be found in References 8 and 9.

DESIGN ASSUMPTIONS

Fig. 2 shows the lateral load deflected shape of a precast concrete wall with vertical joint connectors. The forces that develop in each panel as the wall is deformed laterally are shown in Fig. 3. The following design assumptions were made:

1. Wall panels undergo in-plane axial, flexural, and shear deformations only. Torsional and out-of-plane deformations are not considered.

2. Seismic forces at each floor and at the roof are transferred to the wall panels by floor and roof diaphragms through adequate connections between the wall panels and the diaphragms, enabling the panels to pivot about their own neutral axis. The diaphragms are assumed to be rigid for in-plane forces.

3. All wall panels undergo the same displacements at each floor and roof level based on the rigid floor and roof diaphragm assumption.

4. Vertical joint connectors have elastic-perfectly-plastic shear force deformation characteristics, with adequate ductility to remain fully functional during the seismic response of the wall. No horizontal tension or compression forces are transferred between panels across vertical joints, based on the rigid floor and roof diaphragm assumption. All vertical joints use the same number of vertical joint connectors, and have identical geometry and material properties.

5. Anchorages of the post-tensioning steel and of the vertical joint connectors remain fully effective during the seismic response of the wall.

6. Elastic and inelastic deformations that may occur in the foundation or the supporting ground are not considered.

7. The wall is adequately braced against out-of-plane buckling.

DESCRIPTION OF WALL PARAMETERS

The forces acting on selected panels of a wall that is composed of an arbitrary number of panels and floor levels are shown in Fig. 3. The letter k represents the panel number, ranging from 1 to n, where n is the total number of panels in a wall. The letter i represents the floor level, ranging from 1 to r, where r represents the total number of floor levels supported by a wall. The length along the base of each panel is denoted by l_x. Therefore, the length along the base of the wall, l_w, is the product of n and l_x. H_w and t_w are the height and thickness of the wall, respectively, and are the same for all panels, as is the length.

As shown in Fig. 3, the height of each floor level, H_i, can be expressed as a fraction of the total wall height, H_w, by:

$$H_i = r_{Hi} H_w \tag{1}$$

where r_{Hi} is the ratio of the height of floor level i to the wall height. The height of the roof level H_r is calculated using Eq. (1) with $i = r$. Since the height of the roof level is the height of the wall, $r_{Hr} = 1$ and $H_r = H_w$, as shown in Fig. 3.

Fig. 3 also shows the forces that act on each panel under lateral load. These forces are (1) floor and roof lateral loads transmitted to the panels by the floor and roof diaphragms ($F_{k,i}$ and $F_{k,r}$), (2) a panel base shear force that is in horizontal equilibrium with the panel lateral loads (V_k), (3) a gravity force that accounts for floor and roof loads as well as the panel self-weight (N_k), (4) post-tensioning forces (T_1 and T_2), (5) a concrete compression stress resultant at the base (C_k), and (6) the total shear force that is transferred into the panel across the vertical joint connectors (P_j).

In Fig. 3, the lateral force acting at an arbitrary level of a given panel is defined as $F_{k,i}$, where k is the panel number and i is the floor level. This notation is used because the floor and roof lateral loads may be different for each panel.

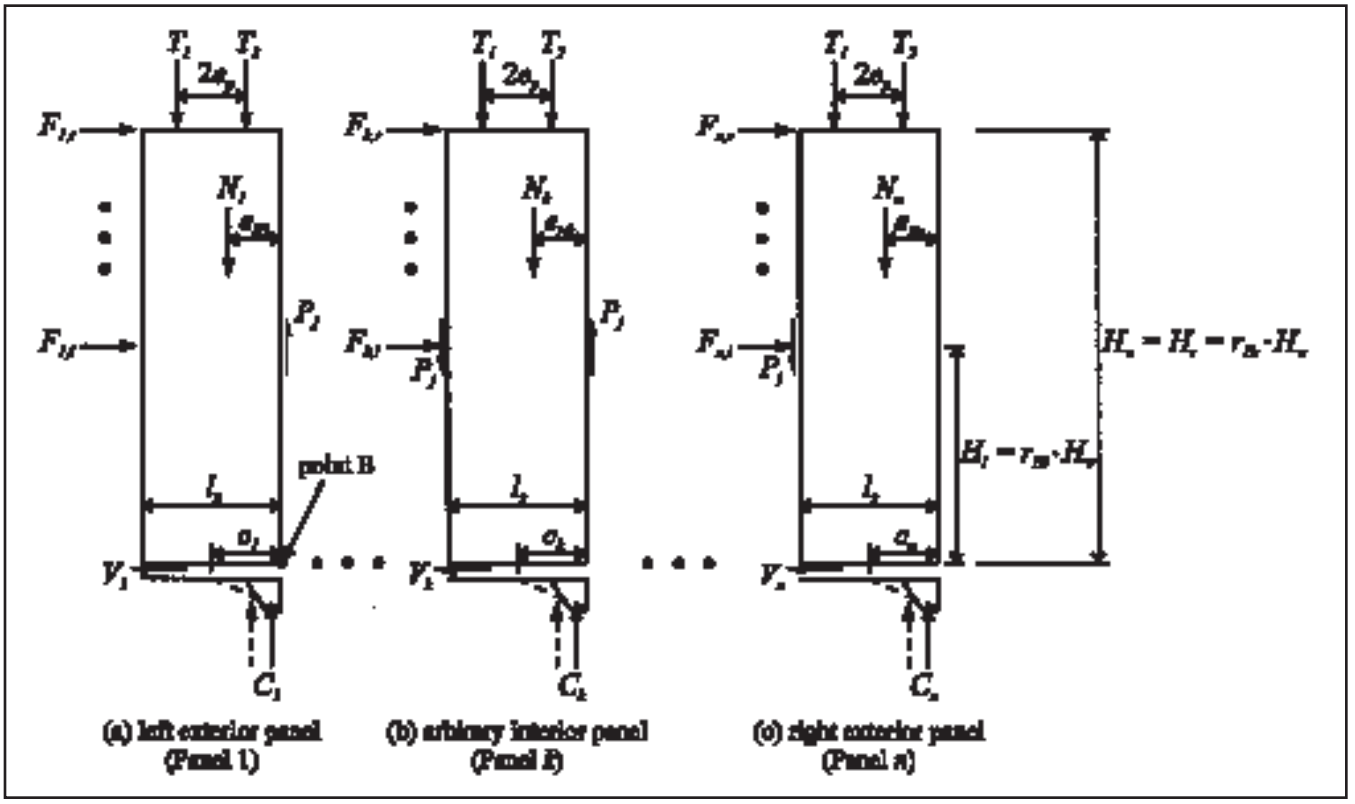

Fig. 3. Forces on each panel of an unbonded post-tensioned precast concrete wall.

Fig. 4 shows that the lateral force acting on the wall at the roof level, $F_{w,r}$, is expressed as the sum of the panel forces at that level, $\Sigma F_{k,r}$, where $k = 1$ to n. $F_{w,r}$ is further expressed as a fraction of the total base shear of the wall, V_w, by:

$$F_{w,r} = r_{Fr} V_w \tag{2}$$

where r_{Fr} is the fraction of the total base shear applied at the roof level. Similarly, the lateral force on the wall at floor level i can be expressed as:

$$F_{w,i} = r_{Fi} V_w \tag{3}$$

where r_{Fi} is the fraction of the total base shear applied at floor level i (Fig. 4). The wall base shear, V_w in Eqs. (2) and (3), is equal to the sum of the panel base shears, ΣV_k, where $k = 1$ to n (Fig. 4).

Referring to Figs. 3 and 4, the gravity force on a panel, including the panel self-weight, is N_k. This force acts at an eccentricity e_{Nk} measured from the *right* edge of the panel. The gravity force and the eccentricity may vary for each panel. T_1 and T_2 are the post-tensioning forces acting on groups of post-tensioning steel toward the *left* edge and toward the *right* edge of each panel, respectively. T_{1i} and T_{2i} represent the initial prestress force in the group of post-tensioning steel toward the *left* edge and toward the *right* edge of each panel, respectively, after the application of prestress forces and gravity loads on the wall.

Note that T_1 and T_2 in Figs. 3 and 4 may differ from each other, but each panel is subjected to the same values of T_1 and T_2. The two groups of post-tensioning steel in a panel are a distance of $2e_p$ apart, where e_p is the eccentricity of the post-tensioning steel measured from the centerline of the panel to the centroid of the group of steel. The eccentricity of the post-tensioning steel is constant for all panels.

The compression stress resultant acting at the base of an arbitrary panel k is defined by C_k (see Figs. 3 and 4). The compression stress resultant after the application of prestress forces and gravity loads, but prior to the application of lateral loads on a panel, is defined as C_{ki}. The length of the compression block at the base of the panel is c_k. Figs. 3 and 4 illustrate two compression stress distributions at the base of each panel (represented by a dashed and a solid line) and the corresponding locations of the compression stress resultant. The stress distribution represented by the dashed line is a linear stress distribution which corresponds to a state in the lateral load response of the wall where the gaps at the horizontal joint at the base of each panel have propagated beyond the centerline of the wall panels (see Fig. 2), but the concrete at the compression end of each panel remains in the elastic range.

As discussed later, this linear stress distribution is assumed when calculating the wall base shear corresponding to the effective linear limit state, V_{ell} [Eq. (4)]. The stress distribution represented by the solid line in Figs. 3 and 4 corresponds to a state in the lateral load response of the wall where nonlinear behavior in the concrete at the compression end of each panel occurs after significant gap opening of the horizontal joint at the base. A nonlinear stress distribution is assumed when calculating the wall base shear corresponding to yielding of the post-tensioning steel, V_{llp} [Eq. (11)].

A wall may have numerous vertical joint connectors

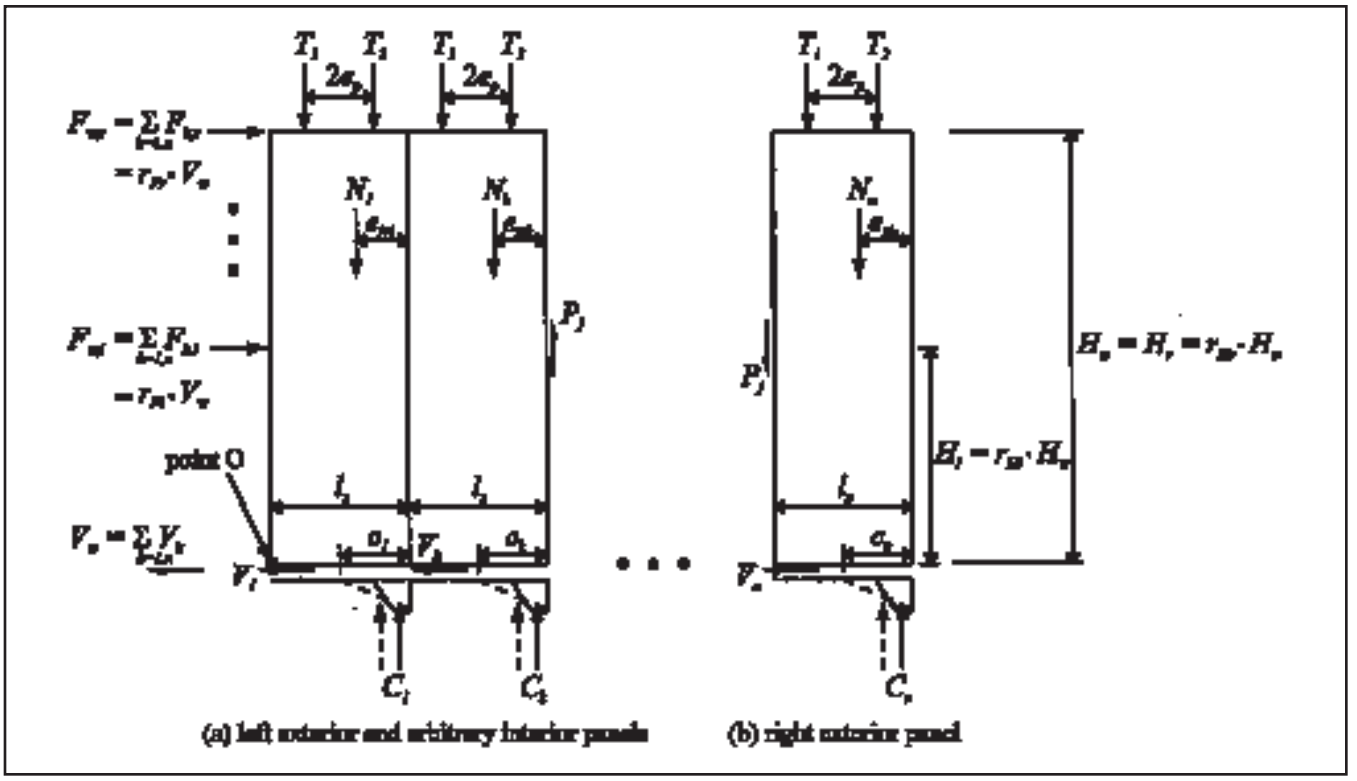

Fig. 4. Forces on an unbonded post-tensioned precast concrete wall with multiple panels.

transferring shear across a given vertical joint. However, only the *total* shear force transferred between panels across a vertical joint (P_j in Figs. 3 and 4) is considered.

This paper presents the derivation of closed-form expressions that are used to estimate various capacities of an unbonded post-tensioned precast concrete wall under combined gravity and lateral loads. The closed-form expressions are derived using free-body diagrams similar to those shown in Figs. 3 and 4, and consider a wall that is loaded laterally to the *right*, causing the wall to displace to the *right*. For a wall that is loaded to the *right*, the locations of T_1 and T_2, and the location of N (defined by e_N), are as defined above. However, if the lateral loads are applied to the *left* (a case that should be considered for a wall with different prestress forces, T_1 and T_2, or with eccentric gravity loads, N), then the closed-form expressions are still valid as long as T_1 and T_2 are interchanged and e_N is measured from the *left* edge of the panels.

TRILINEAR IDEALIZED LATERAL LOAD BEHAVIOR

The idealized lateral load behavior of an unbonded post-tensioned precast concrete wall with vertical joints and ductile connectors is presented below and is defined using a trilinear load-displacement response curve.

Wall Limit States

The limit states considered for unbonded post-tensioned precast concrete walls are introduced using the idealized lateral load behavior shown in Fig. 5. The limit states are (1) decompression at the base of the wall (DEC), (2) yielding of vertical joint connectors (LLJ), (3) effective limit of the linear-elastic response of the wall (ELL), (4) yielding of post-tensioning steel (LLP), (5) base shear capacity, (6) loss of prestress under cyclic lateral load, (7) crushing of confined concrete (CCC), and (8) fracture of post-tensioning steel. These limit states are described below. Limit States 3 (ELL), 4 (LLP), and 7 (CCC) define the trilinear idealized lateral load behavior shown in Fig. 5.

Decompression — Decompression at the base of the wall occurs when the precompression due to post-tensioning and gravity loads is reduced to zero at one edge of the base of a wall panel by the overturning moment due to lateral loads. Since the wall comprises multiple panels, this limit state is defined as the first occurrence of decompression in any of the wall panels. Under a specified lateral load distribution, decompression of the wall can be related to a specific level of base shear and roof displacement, V_{dec} and Δ_{dec}, respectively. Decompression is accompanied by the initiation of gap opening along the horizontal joint at the base of the wall. V_{dec} and Δ_{dec} can be determined from nonlinear lateral load analyses using the fiber model described in the companion paper.[1]

Yielding of vertical joint connectors — The walls examined in this study employ ductile connectors along the vertical joints. Vertical joint connectors are intended to yield in shear. Since a wall may contain several vertical joints, this limit state is defined as the first occurrence of yielding of the vertical joint connectors across one vertical joint. The base shear and roof displacement corresponding to the shear yield strain of the vertical joint connectors are designated V_{llj} and Δ_{llj}, respectively. V_{llj} and Δ_{llj} can be determined from

nonlinear lateral load analyses using the fiber model described in the companion paper.[1]

Effective linear limit — The lateral load response of a wall is essentially linear elastic immediately after decompression. With continued displacement, however, a substantial reduction in lateral stiffness (called softening) results from the progression of gap opening along the horizontal joints at the base of the wall. The point at which the softening is apparent is referred to as the effective linear limit. The base shear and roof displacement corresponding to the effective linear limit are denoted as V_{ell} and Δ_{ell}, respectively. Since the softening usually develops in a smooth and continuous manner,[3] the term *effective* linear limit is used to describe this point on the lateral load response of a wall. As a result of the smooth softening behavior, there is no specific stress condition associated with this point. V_{ell} and Δ_{ell} are estimated using closed-form expressions derived later.

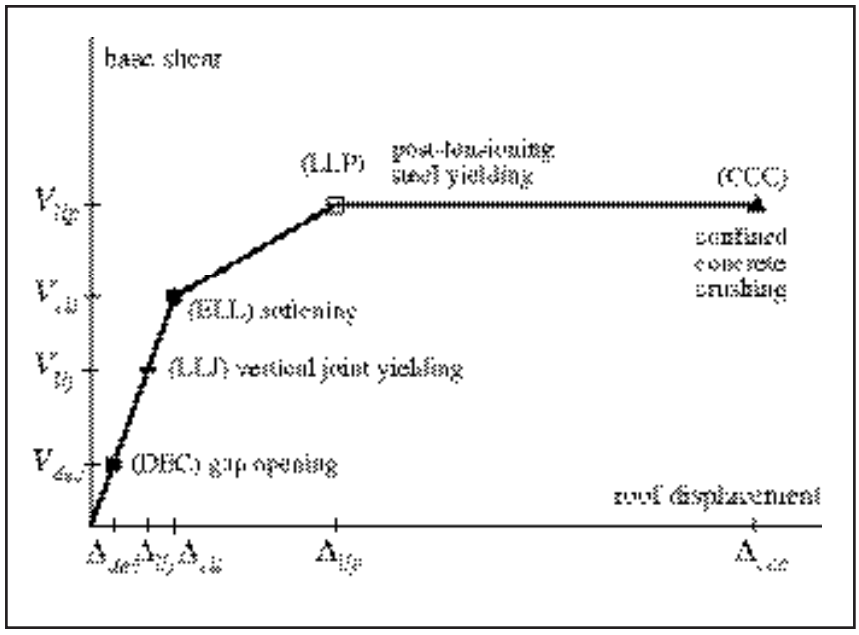

Fig. 5. Wall limit states.

Yielding of post-tensioning steel — Yielding of the post-tensioning steel occurs when the strain reaches the yield strain of the steel. For the walls considered in this study, the post-tensioning steel does not yield simultaneously in all the panels. Therefore, this limit state is defined as the first occurrence of yielding in the post-tensioning steel. The base shear and roof displacement corresponding to yielding of the post-tensioning steel are denoted as V_{llp} and Δ_{llp}, respectively. Due to unbonding, the yield strain of the post-tensioning steel is usually reached after the effective linear limit is reached (and thus after significant softening occurs).[3] V_{llp} and Δ_{llp} are estimated using closed-form expressions derived later, and can be determined accurately from nonlinear lateral load analyses using the fiber model described in the companion paper.[1]

Base shear capacity — The base shear capacity of a wall is intended to be controlled by axial-flexural behavior rather than by shear sliding at the base. Thus, at this limit state, the overturning capacity of a wall controls the base shear capacity. The idealized lateral load behavior shown in Fig. 5 neglects strain-hardening effects in the post-tensioning steel. As a result, the base shear capacity of the wall is assumed to equal the base shear at the first occurrence of yielding in the post-tensioning steel. Therefore, the base shear capacity equals V_{llp}, and the corresponding roof displacement is Δ_{llp}.

Loss of prestress — Prestress will be lost in an unbonded post-tensioned wall under cyclic lateral load when the wall is unloaded from a drift that has exceeded the drift at which the post-tensioning steel yields. This is illustrated in Fig. 6, which shows a typical prestressing steel stress-strain relationship. f_{pi} is the initial stress in the post-tensioning steel after the application of prestress forces and gravity loads on the wall. If the steel strain remains elastic during cyclic lateral loading of the wall, no loss of prestress will result (neglecting inelastic deformations that may occur in the concrete in a highly stressed wall). If the steel strain exceeds the yield strain, as does Point 2 in Fig. 6, some prestress will be lost after the lateral load is removed, since the steel unloads elastically from Point 2. Hence, after the lateral load is removed from the wall, the prestress is reduced from f_{pi} to a residual value f_{pr}. Upon unloading from an even larger inelastic strain, such as Point 3 in Fig. 6, the entire prestress may be lost.

Crushing of confined concrete — Failure of a wall occurs when the confined concrete at the base of the panels fails in compression. Based on the concrete confinement model developed by Mander et al.[11,12] crushing of the confined concrete occurs at an ultimate concrete compressive strain ε_{cu} that is reached when the confining reinforcement fractures. Significant loss of lateral load and gravity load resistance is expected to occur when crushing of the confined concrete occurs. The base shear and roof displacement corresponding to crushing of the confined concrete are denoted as V_{ccc} and Δ_{ccc}, respectively. V_{ccc} and Δ_{ccc} can be determined from nonlinear lateral load analyses using the fiber model described in the companion paper.[1]

Fracture of post-tensioning steel — Fracture of the post-tensioning steel occurs when the strain reaches the maximum strain of the steel. Significant loss of lateral load resistance as well as loss of self-centering capability is expected to occur at fracture of the post-tensioning steel. The roof displacement corresponding to fracture of the post-tensioning steel is denoted as Δ_{fp}. Δ_{fp} can be determined from nonlinear lateral load analyses using the fiber model described in the companion paper.[1]

ESTIMATION OF WALL CAPACITIES

This section derives expressions that estimate the base shear and roof displacement capacities corresponding to

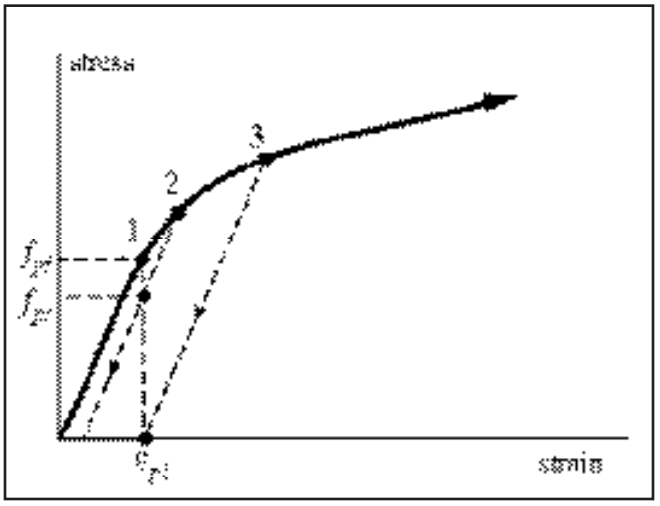

Fig. 6. Prestress loss due to inelastic response (adapted from Priestley and Tao[10]).

Points ELL and LLP, which partly define the trilinear idealized lateral load behavior shown in Fig. 5. Expressions are derived for the general case of an unbonded post-tensioned precast concrete wall with *n* panels, *r* stories, and eccentric gravity forces as shown in Figs. 3 and 4. In addition, expressions are derived for the specific case of the prototype wall (considered in the design example presented later), with three panels, two stories, and concentric gravity forces.

Base Shear at the Effective Linear Limit State, V_{ell}

A one-panel-wide unbonded post-tensioned precast concrete wall has been shown to reach the effective linear limit state when the base moment (which is in equilibrium with the applied lateral loads, the initial prestress forces, and the gravity load) is between $2M_{dec}$ and $3M_{dec}$, where M_{dec} is the base moment corresponding to the decompression limit state.[3,13] Taking the effective linear limit at a base moment equal to $2.5M_{dec}$, and assuming a linear stress distribution along the compression region of the base of the one-panel-wide wall, the length of the compression region along the horizontal joint at the base is equal to one-fourth of the panel length ($0.25l_x$).

This means that the gap at the base is assumed to have propagated to 0.75 times the panel length ($0.75l_x$) at the effective linear limit state. This result can be applied to an unbonded post-tensioned precast concrete wall with an arbitrary number of panels and with vertical joint connectors. Assuming that the lengths of the compression regions of the middle panels and the average length of the compression regions of the two exterior panels are $0.25l_x$ and summing moments about the extreme tension edge of the base of the left exterior panel (Point O in Fig. 4), the base shear corresponding to the effective linear limit state, V_{ell}, can be estimated for a wall with *n* panels, *r* stories, and eccentric gravity forces by:

$$V_{ell} = \frac{A_{ell} + B_{ell} + \sum_{k=2,n-1} C_{ell,k}}{H_w \sum_{i=1,r} (r_{Hi} r_{Fi})} \qquad (4)$$

where

$$A_{ell} = -T_1\left(\frac{l_x}{2} - e_p\right) - T_2\left(\frac{l_x}{2} + e_p\right) - N_1(l_x - e_{N1}) + C_1\left(l_x - \frac{c_1}{3}\right)$$

$$B_{ell} = -T_1\left[(n-1)l_x + \frac{l_x}{2} - e_p\right] - T_2\left[(n-1)l_x + \frac{l_x}{2} + e_p\right] - N_n(nl_x - e_{Nn}) + C_n\left(nl_x - \frac{c_n}{3}\right)$$

$$C_{ell,k} = -T_1\left[(k-1)l_x + \frac{l_x}{2} - e_p\right] - T_2\left[(k-1)l_x + \frac{l_x}{2} + e_p\right] - N_k(kl_x - e_{Nk}) + C_k\left(kl_x - \frac{c_k}{3}\right)$$

$$c_1 = \frac{l_x\sqrt{C_1}}{2\left(\sqrt{C_1} + \sqrt{C_n}\right)}$$

$$c_n = \frac{l_x\sqrt{C_n}}{2\left(\sqrt{C_1} + \sqrt{C_n}\right)}$$

$$c_k = \frac{l_x\sqrt{C_k}}{2\left(\sqrt{C_1} + \sqrt{C_n}\right)}$$

$$C_1 = N_1 + T_1 + T_2 - P_j$$

$$C_n = N_n + T_1 + T_2 + P_j$$

$$C_k = N_k + T_1 + T_2$$

$$P_j = P_{llj}$$

$$T_1 = T_{1i}$$

$$T_2 = T_{2i}$$

A_{ell}, B_{ell}, and $C_{ell,k}$ represent the sum of moments about Point O in Fig. 4 for the left exterior panel (Panel 1), the right exterior panel (Panel *n*), and an interior panel (Panel *k*), respectively, which, when added over all the panels, is in equilibrium with the overturning moment caused by the applied lateral loads. For a wall with one panel, B_{ell} and $\Sigma C_{ell,k}$ are zero. For a wall with only two panels, $\Sigma C_{ell,k}$ is zero (no interior panels). A wall with three or more panels involves A_{ell}, B_{ell}, and $\Sigma C_{ell,k}$.

C_1, C_n, and C_k are the compression resultants at the base of the left exterior panel, the right exterior panel, and the interior panels, respectively. C_1, C_n, and C_k act at a distance $c_1/3$, $c_n/3$, and $c_k/3$ from the right edge of each panel, respectively, corresponding to a linear compressive stress distribution (represented by a dashed line in Fig. 4). C_1, C_n, and C_k are in equilibrium with the gravity force, N_k, where $k = 1$ to *n*, prestress forces, T_1 and T_2, and the vertical joint shear force, P_j.

T_1 and T_2 are assumed to be equal to the initial prestress force on the steel, T_{1i} and T_{2i}, respectively, which are the same for all panels. P_{llj} is the total shear yield force in the vertical joint connectors. Vertical joint connectors are assumed to be yielding when the effective linear limit state of the wall is reached, because at this state the gap at the tension side of the panels has opened significantly, producing

relative displacements between adjacent panels that are large enough for yielding of the connectors in shear. (This assumption may not be valid if vertical joint connectors with very large shear yield deformation capacities are used.) A limit on the shear yield deformation capacity of the vertical joint connectors is given below.

The following explains the derivation of the term in the denominator of Eq. (4). First, the lateral force on the wall at each floor level, $F_{w,i}$ (shown in Fig. 4), is taken as the sum of the panel forces, $F_{k,i}$, on that floor level (Fig. 3). The lateral force on the wall at each floor level is then expressed as a fraction of the total base shear of the wall, V_w (see Fig. 4), by Eq. (3), with $V_w = V_{ell}$. Similarly, the total force on the wall at the roof level is expressed as a fraction of the total base shear of the wall by Eq. (2), with $V_w = V_{ell}$. The height of each floor level and the height of the roof level, measured from the base of the wall, are expressed as a fraction of the total wall height, H_w, by Eq. (1), where $i = 1$ to r and $r_{Hr} = 1$. Summing moments about Point O in Fig. 4, the overturning moment caused by the applied lateral loads (measured positive in the clockwise direction) that is in equilibrium with A_{ell}, B_{ell}, and $\Sigma C_{ell,k}$ is written as:

$$M_{ell} = \sum_{i=1,r} \left(r_{Hi} H_w\right)\left(r_{Fi} V_{ell}\right) \tag{5}$$

From equilibrium, Eq. (5) is equal to the sum of A_{ell}, B_{ell}, and $\Sigma C_{ell,k}$. Thus, factoring V_{ell} from Eq. (5) and dividing through by the summation term yields Eq. (4).

Eq. (4) is derived for a wall that has lateral loads applied to the right, as shown in Fig. 4. If the lateral loads are applied to the left, Eq. (4) is valid as long as T_1 and T_2 are interchanged, e_N is measured from the *left* edge of the panels, and M_{ell} is measured positive in the *counter-clockwise* direction.

For the prototype wall considered in the design example, composed of two stories, three panels with the same geometry, the same gravity forces, N, acting at the center of each panel, and the forces T_1 and T_2 each equal to half the total initial prestress force on a panel, Eq. (4) becomes:

$$V_{ell} = \frac{l_x\left[\sqrt{C_1}\left(13P_j + 8C_2\right) + \sqrt{C_3}\left(11P_j + 8C_2\right) - \sqrt{C_2 C_2}\right]}{6H_w\left(r_{H1} r_{F1} + r_{Hr} r_{Fr}\right)\left(\sqrt{C_1} + \sqrt{C_3}\right)} \tag{6}$$

where

$C_1 = N + P_i - P_j$
$C_2 = P_i + N$
$C_3 = P_i + N + P_j$
$P_j = P_{llj}$
$T_1 = T_2 = P_i/2$

C_1, C_2, and C_3 are the compression resultants at the base of the left exterior panel (Panel 1), the interior panel (Panel 2), and the right exterior panel (Panel 3), respectively, which are in equilibrium with the gravity force N, total prestress force on a panel P_i, and the vertical joint shear force P_j. The values r_{Fi}, r_{F1}, and r_{Fr} in Eqs. (4) and (6) are determined from the vertical distribution of seismic forces in accordance with an applicable building code, such as NEHRP,[14] UBC,[15] or IBC.[16]

Roof Displacement at the Effective Linear Limit State, Δ_{ell}

To estimate the roof displacement corresponding to the effective linear limit state, Δ_{ell}, the wall is modeled as a cantilever beam subjected to lateral loads at each floor level and concentrated moments produced by eccentric gravity forces at each floor level. The uncracked elastic section properties of the wall are obtained by calculating the properties of one panel and multiplying them by the total number of panels, n, in the wall. The resulting bending and shear deformations are then computed.

The stiffness of the vertical joint connectors is neglected in the derivation of Δ_{ell} for simplicity; this does not imply, however, that the stiffness of the vertical joint connectors is small enough to be neglected. The effect of neglecting the initial stiffness of the vertical joint connectors on the derivation of Δ_{ell} is studied in the companion paper.[1] Gap opening at the base of the wall is neglected, since Δ_{ell} is an estimate of the roof displacement when gap opening begins to appreciably affect the stiffness.

An elastic analysis of a wall with r stories, n panels of the same geometry with eccentric gravity forces on each panel that can vary along the height of the wall, and lateral loads applied at each floor level gives the following estimation of the roof displacement corresponding to the effective linear limit state:

$$\Delta_{ell} = \Delta_{Fr} + \Delta_{Sr} + \Delta_{Nr} + \Delta_{Pr} \tag{7}$$

where

$$\Delta_{Fr} = \sum_{i=1,r} \frac{1}{2E_c I_w}\left(r_{Fi} V_{ell}\right) {r_{Hi}}^2 {H_w}^3 \left(r_{Hr} - \frac{1}{3} r_{Hi}\right)$$

$$\Delta_{Sr} = \sum_{i=1,r} \frac{1}{G_c A'_w}\left(r_{Fi} V_{ell} r_{Hi} H_w\right)$$

$$\Delta_{Nr} = \sum_{i=1,r} \frac{1}{E_c I_w} M_{w,i}\left(r_{Hi} H_w\right) H_w \left(r_{Hr} - \frac{1}{2} r_{Hi}\right)$$

$$\Delta_{Pr} = \frac{n e_p (T_2 - T_1) {H_w}^2}{2E_c I_w}$$

$$T_1 = T_{1i}$$

$$T_2 = T_{2i}$$

Δ_{Fr} is the elastic roof deflection of the wall in flexure due to lateral forces. Δ_{Fr} is obtained using the principle of superposition (successively applying a concentrated lateral load, $r_{Fi}V_{ell}$, along the height of the wall and adding the corresponding roof deflections). The roof deflection of the wall due to elastic shear deformations, similarly obtained using the principle of superposition, is denoted as Δ_{Sr}. Δ_{Nr} is the elastic roof deflection of the wall in flexure due to the eccentric gravity forces. The notation $M_{w,i}$ in the Δ_{Nr} equation represents a concentrated wall moment (measured positive in the clockwise direction) at floor level i, which is derived using a wall as shown in Fig. 3. The total gravity load of

each panel, N_k, is represented by a gravity load at each floor level, $N_{k,i}$, and a gravity load at the roof level, $N_{k,r}$.

The eccentricities at which the gravity loads are applied, e_{Nk}, measured from the right edge of the panels are the same along the height of a given panel, but may vary from panel to panel. The eccentric normal gravity force at each level can be replaced by the normal force acting at the center of the panel, plus a concentrated moment measured positive in the clockwise direction. Summing the panel concentrated moments due to eccentric gravity loads across all panels at a particular floor level yields a concentrated moment in the wall at that level. In general, the concentrated wall moment (measured positive in the clockwise direction) at floor level *i* is given by:

$$M_{w,i} = \sum_{k=1,n} N_{k,i}\left(\frac{l_x}{2} - e_{Nk}\right) \tag{8}$$

Similarly, the concentrated wall moment (measured positive in the clockwise direction) at the roof level (level *r*) is given by:

$$M_{w,r} = \sum_{k=1,n} N_{k,r}\left(\frac{l_x}{2} - e_{Nk}\right) \tag{9}$$

In Eq. (7), Δ_{Pr} is the elastic roof deflection of the wall caused by the application of different initial prestress forces in the left post-tensioning steel group and the right post-tensioning steel group of each panel, denoted by T_{1i} and T_{2i}, respectively. The initial prestress forces, T_{1i} and T_{2i}, are assumed to be the same for all panels. The moment produced by the unbalanced prestress forces on a panel is added over the panels and is applied to the wall as a concentrated moment (measured positive in the clockwise direction) at the roof level because, since the post-tensioning steel is unbonded over the entire height of the wall, the wall is subjected to a constant moment over its entire height.

V_{ell} in Eq. (7) is found from Eq. (4). G_c is the shear modulus of concrete, A'_w is the effective shear area of the wall, E_c is the elastic modulus of concrete, and I_w is the moment of inertia of the uncracked transformed section of the wall.

Eq. (7) is derived for a wall that has lateral loads applied to the right, as shown in Fig. 3. If the lateral loads are applied to the left, Eq. (7) is valid as long as T_1 and T_2 are interchanged, e_N is measured from the *left* edge of the panels, $M_{w,i}$ and $M_{w,r}$ are both measured positive in the *counter-clockwise* direction, and the concentrated wall moment produced by unbalanced prestress forces on the panels is measured positive in the *counter-clockwise* direction.

For the prototype wall composed of two stories, three panels with the same geometry, the same gravity forces *N* acting at the center of each panel, and the same forces T_1 and T_2 each equal to half the total initial prestress force on a panel, Eq. (7) becomes:

$$\Delta_{ell} = \Delta_{Fr} + \Delta_{Sr} \tag{10}$$

where

$$\Delta_{Fr} = \frac{1}{2E_cI_w}\left[(r_{F1}V_{ell})r_{H1}{}^2H_w{}^3\left(r_{Hr} - \frac{1}{3}r_{H1}\right) + (r_{Fr}V_{ell})r_{Hr}{}^2H_w{}^3\left(r_{Hr} - \frac{1}{3}r_{Hr}\right)\right]$$

$$\Delta_{Sr} = \frac{1}{G_cA'_w}\left(r_{F1}V_{ell}r_{H1}H_w + r_{Fr}V_{ell}r_{Hr}H_w\right)$$

The notation Δ_{Fr} is the elastic roof deflection of the wall in flexure due to lateral forces, and Δ_{Sr} is the roof deflection of the wall due to elastic shear deformations. V_{ell} in Eq. (10) is computed using Eq. (6). The values of r_{Fi}, r_{F1}, and r_{Fr} in Eqs. (7) and (10) are determined from a code-specified distribution of equivalent lateral forces.

Note that V_{ell} is based on gap opening in flexure along the base of the wall (recall that the length of the gaps at the base of the interior panels and the average length of the gaps at the base of the two exterior panels are assumed to be $0.75l_x$), while Δ_{ell} is calculated from elastic deformations of the wall without considering gap opening. The estimate of Δ_{ell} is considered to be reasonable because the effect of gap opening on the lateral displacement of the wall is small until V_{ell} is reached.

From earlier discussion, the vertical joint connectors are assumed to be yielded [$P_j = P_{llj}$ in Eq. (4)] at the effective linear limit state (ELL in Fig. 5). Therefore, to ensure the validity of this assumption, a limit must be imposed on the shear yield deformation capacity of the vertical joint connectors. This limit can be defined as the relative vertical displacement between adjacent panels along the vertical joints at the effective linear limit state, $\Delta_{v,ell}$.

$\Delta_{v,ell}$ is derived by establishing a kinematic relationship between the horizontal displacement of a panel at the roof level (Δ_{ell}) and the vertical displacement of the panel at its tension edge ($\Delta_{v,ell}$) as the panel pivots rigidly about the neutral axis location ($0.75l_x$ measured from the tension edge of the panel). The result is $\Delta_{v,ell} = 0.75l_x\Delta_{ell}/H_w$. Therefore, the equations derived above for V_{ell} and Δ_{ell} are valid when the shear yield deformation capacity of the vertical joint connectors is less than $\Delta_{v,ell}$.

Base Shear at Yielding of Post-Tensioning Steel, V_{llp}

The base shear corresponding to yielding of the post-tensioning steel, V_{llp}, is derived for a wall with *n* panels, *r* stories, and eccentric gravity forces, N_k, using the free body diagram shown in Fig. 4 and is given as:

$$V_{llp} = \frac{A_{llp} + B_{llp} + \sum_{k=2,n-1} C_{llp,k}}{H_w \sum_{i=1,r}(r_{Hi}r_{Fi})} \tag{11}$$

where

$$A_{llp} = -T_1\left(\frac{l_x}{2} - e_p\right) - T_2\left(\frac{l_x}{2} + e_p\right) - N_1\left(l_x - e_{N1}\right) + C_1\left(l_x - \frac{l_x}{30}\right)$$

$$B_{llp} = -T_1\left[(n-1)l_x + \frac{l_x}{2} - e_p\right] - T_2\left[(n-1)l_x + \frac{l_x}{2} + e_p\right] - N_n\left(nl_x - e_{Nn}\right) + C_n\left(nl_x - \frac{l_x}{30}\right)$$

$$C_{llp,k} = -T_1\left[(k-1)l_x + \frac{l_x}{2} - e_p\right] - T_2\left[(k-1)l_x + \frac{l_x}{2} + e_p\right] - N_k\left(kl_x - e_{Nk}\right) + C_k\left(kl_x - \frac{l_x}{30}\right)$$

$$C_1 = N_1 + T_1 + T_2 - P_j$$

$$C_n = N_n + T_1 + T_2 + P_j$$

$$C_k = N_k + T_1 + T_2$$

$$P_j = P_{llj}$$

$$T_1 = T_{llp}$$

$$T_2 = T_{2i}$$

The notation A_{llp}, B_{llp}, and $C_{llp,k}$ represent the sum of moments about Point O in Fig. 4 for the left exterior panel (Panel 1), the right exterior panel (Panel *n*), and an interior panel (Panel *k*), respectively; when added over all the panels, the moment sum is in equilibrium with the overturning moment caused by the applied lateral loads. For a wall with one panel, B_{llp} and $\Sigma C_{llp,k}$ are zero. For a wall with only two panels, $\Sigma C_{llp,k}$ is zero (no interior panels). A wall with three or more panels involves A_{llp}, B_{llp}, and $\Sigma C_{llp,k}$.

The notation C_1, C_n, and C_k are the compression resultants at the base of the left exterior panel, the right exterior panel, and the interior panels, respectively. The compression resultants C_1, C_n, and C_k are located at a distance $l_x/30$ from the right edge of each panel, and correspond to a nonlinear compressive stress distribution (represented by a solid line in Fig. 4). The value of $l_x/30$ is based on results from a fiber-based analytical model described in the companion paper.[1] The values C_1, C_n, and C_k are in equilibrium with the gravity force, N_k, where $k = 1$ to n, prestress forces, T_1 and T_2, and the vertical joint shear force, P_j. T_{llp} represents the force in the post-tensioning steel when it reaches its yield strain. T_{2i} represents the initial prestress force in the post-tensioning steel.

At the limit state under consideration (i.e., LLP in Fig. 5), $P_j = P_{llj}$, is based on the assumed elastic-perfectly-plastic shear force-deformation characteristics of the vertical joint connectors. In addition, the force in the post-tensioning steel group located toward the left edge of the panels, T_1 (see Fig. 4), equals T_{llp}, while the force in the steel group toward the right edge is assumed to equal the initial prestress force, T_{2i}. Thus, since T_{llp} is larger than T_{1i} and $P_j = P_{llj}$, the compression stress resultants C_1, C_n, and C_k are larger in Eq. (11) (at LLP) than in Eq. (4) (at ELL).

The denominator of Eq. (11) is derived in the same way as the denominator of Eq. (4) is derived. First, the lateral force on the wall at each floor level, $F_{w,i}$ (shown in Fig. 4), is taken as the sum of the panel forces, $F_{k,i}$, on that floor level (Fig. 3). The lateral force on the wall at each floor level is then expressed as a fraction of the total base shear of the wall, V_w (see Fig. 4), by Eq. (3), with $V_w = V_{llp}$. Similarly, the total force on the wall at the roof level is expressed as a fraction of the total base shear of the wall by Eq. (2), with $V_w = V_{llp}$. The height of each floor level and the height of the roof level, measured from the base of the wall, are expressed as a fraction of the total wall height, H_w by Eq. (1), where $i = 1$ to r and $r_{Hr} = 1$. Summing moments about Point O in Fig. 4, the overturning moment caused by the applied lateral loads (measured positive in the clockwise direction) that is in equilibrium with A_{llp}, B_{llp}, and $\Sigma C_{llp,k}$ is written as:

$$M_{llp} = \sum_{i=1,r}\left(r_{Hi}H_w\right)\left(r_{Fi}V_{llp}\right) \qquad (12)$$

From equilibrium, Eq. (12) is equal to the sum of A_{llp}, B_{llp}, and $\Sigma C_{llp,k}$. Thus, factoring V_{llp} from Eq. (12) and dividing through by the summation term yields Eq. (11).

Eq. (11) is derived for a wall that has lateral loads applied to the right, as shown in Fig. 4. If the lateral loads are applied to the left, Eq. (11) is valid as long as T_1 and T_2 are interchanged, e_N is measured from the *left* edge of the panels, and M_{llp} is measured positive in the *counter-clockwise* direction.

For the prototype wall considered in the design example, composed of two stories, three panels having the same geometry, and the same gravity forces, N, acting at the center of each panel, Eq. (11) becomes:

$$V_{llp} = \frac{-T_1\left(9\frac{l_x}{2} - 3e_p\right) - T_2\left(9\frac{l_x}{2} + 3e_p\right) - N\left(9\frac{l_x}{2}\right) + C_1\left(\frac{29}{30}l_x\right) + C_2\left(\frac{59}{30}l_x\right) + C_3\left(\frac{89}{30}l_x\right)}{H_w(r_{H1}r_{F1} + r_{Hr}r_{Fr})} \qquad (13)$$

where

$$C_1 = N + T_1 + T_2 - P_j$$

$$C_2 = N + T_1 + T_2$$

$$C_3 = N + T_1 + T_2 + P_j$$

$$P_j = P_{llj}$$

$$T_1 = T_{llp}$$

$$T_2 = T_{2i}$$

C_1, C_2, and C_3 are the compression resultants at the base of the left exterior panel (Panel 1), the middle panel (Panel 2), and the right exterior panel (Panel 3), respectively, which are in equilibrium with the gravity force, N, prestress forces, T_1 and T_2, and the vertical joint shear force, P_j. The values r_{Fi}, r_{F1}, and r_{Fr} in Eqs. (11) and (13) are determined from a code-specified distribution of equivalent lateral forces.

Roof Displacement at Yielding of Post-Tensioning Steel, Δ_{llp}

Consider a wall panel from the precast concrete wall shown in Fig. 3. As presented earlier, the initial stress in the post-tensioning steel after the application of prestress forces and gravity loads on the wall is f_{pi}. When the panel is displaced horizontally at the roof level to its effective linear limit state (Δ_{ell}), the stress in the post-tensioning steel group on the tension edge of the panel is assumed to remain at f_{pi}. Displacement of the roof beyond Δ_{ell} results in a gap opening along the base of the panel until the post-tensioning steel yields.

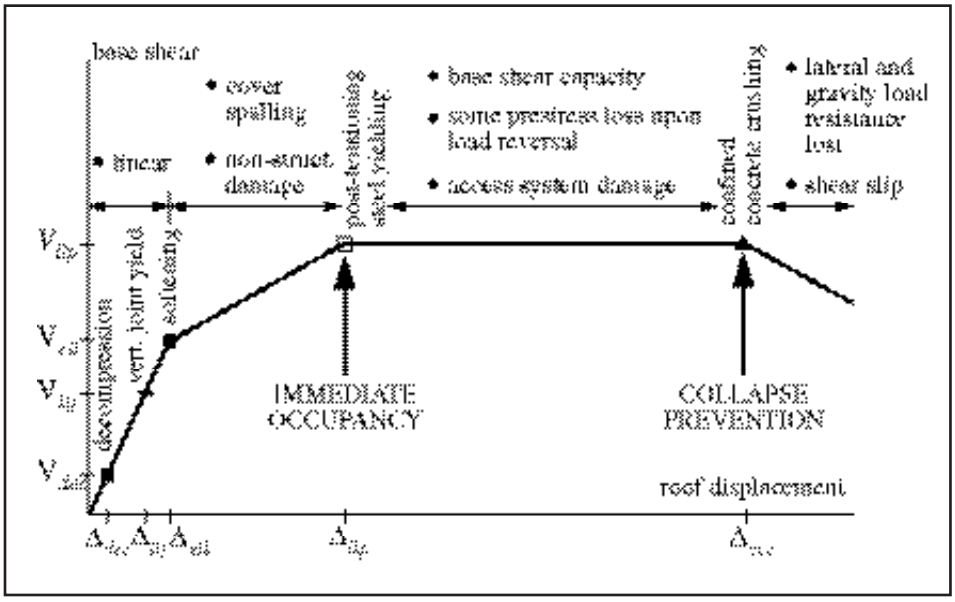

Fig. 7. Structure limit states and expected performance levels (adapted from Kurama et al.[18]).

Thus, the roof displacement when the post-tensioning steel reaches the yield strain is expressed as:

$$\Delta_{llp} = \Delta_{ell} + \Delta_{go} \quad (14)$$

where Δ_{go} is the roof displacement due to the gap opening at the base of the panel. Δ_{ell} is computed from Eq. (7), and Δ_{go} is computed as follows:

$$\Delta_{go} = \frac{2H_w^2\left(f_{pl} - f_{pi}\right)}{E_p\left(l_x + 2e_p\right)} \quad (15)$$

E_p is the modulus of elasticity of the post-tensioning steel and f_{pl} is the yield stress of the post-tensioning steel. Eq. (15) is developed by establishing a kinematic relationship between the horizontal displacement of a panel at the roof level (Δ_{go}) and the vertical displacement of the panel at the location of the post-tensioning steel group on the tension edge of the panel (Δ_v) as the panel pivots rigidly about the compression edge furthest from the applied lateral loads (i.e., Point B in Fig. 3). Δ_v is expressed as the product of the wall height and the change in strain in the post-tensioning steel.

PROPOSED SEISMIC DESIGN APPROACH

Here the authors propose a seismic design approach for building structures that use unbonded post-tensioned precast concrete walls with vertical joints and ductile connectors as the primary lateral load resisting system. The proposed design approach is a performance-based design approach that allows the designer to specify and predict the performance (degree of damage) of a building for a specified level of ground motion intensity. Performance-based design requires identifying (1) performance (damage) levels, (2) structure limit states and capacities, (3) seismic demand levels, and (4) structure demands.

Performance levels — The design approach considers two performance levels that are defined in terms of the maximum damage expected in various structural and non-structural elements during a ground motion. The performance levels, as per FEMA 273,[17] are: (1) the *immediate occupancy* performance level, and (2) the *collapse prevention* performance level. The immediate occupancy performance level refers to a post-earthquake state in which limited structural and non-structural damage occurs. The structure responds to the ground motion in an essentially elastic manner with limited cracking and yielding of structural members. The collapse prevention performance level refers to a post-earthquake damage state where the structure sustains considerable damage and is on the verge of partial or total collapse, but does not collapse.

Structure limit states and capacities — Structure limit states and capacities describe the damage in various structural and non-structural elements of a building. Structure limit states and capacities include limit states and capacities for unbonded post-tensioned precast walls, gravity load resisting frames, and non-structural elements. The limit states for unbonded post-tensioned precast concrete walls with vertical joints and ductile connectors were discussed earlier. The limit state for the gravity load resisting frames is significant loss of gravity load resistance. Kurama et al.[18] assumes that gravity load resisting frames can be designed to sustain a roof drift of 2.5 percent without failure. The same assumption is made in the present study.

The limit states for non-structural elements are (1) initiation of damage to the non-structural elements, and (2) damage to basic access and life safety systems. Damage to non-structural elements occurs when the story drift (relative displacement between adjacent floors) exceeds a certain level. In this research, the story drift is expressed as a percentage of the story height (relative displacement between floors divided by the story height). Freeman[19] indicates that damage to non-structural elements initiates at a story drift of 0.25 percent, while damage requiring repair occurs at a story drift of 0.5 to 1 percent. In the present study, a limit on story drift of 2.0 percent is adopted based on the NEHRP recommended provisions.[14]

Relationship between performance levels and structure limit states — The performance levels and the structure limit states are related using the idealized lateral load response shown in Fig. 7. The immediate occupancy performance level is reached when yielding of the post-tensioning steel occurs (at a roof displacement of Δ_{llp}). Thus, if the displacement response to an earthquake exceeds Δ_{llp}, the result-

ing structural and non-structural damage will likely require some repair before the building can be occupied. The collapse prevention performance level is reached when crushing of the confined concrete occurs (at a roof displacement of Δ_{ccc}). Thus, if the displacement response to an earthquake exceeds Δ_{ccc}, a partial collapse of the building is likely.

Seismic demand levels — Seismic demand levels are generally defined in terms of ground motion levels with selected return periods for a given site. The proposed design approach considers two levels of ground motion: (1) a design level ground motion, and (2) a maximum considered ground motion. The maximum considered ground motion, defined in the NEHRP[14] provisions, has a 2 percent probability of being exceeded in 50 years (corresponding approximately to a 2500-year return period). The design level ground motion is the same as the NEHRP[14] design earthquake ground motion, which has a ground shaking intensity that is two-thirds of the maximum considered earthquake ground motion.

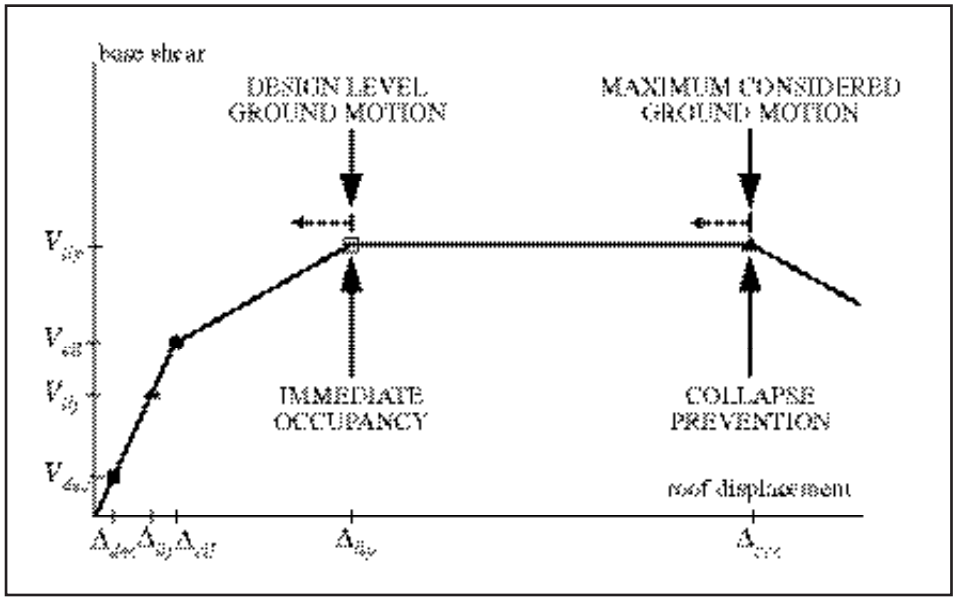

Fig. 8. Objectives of the proposed design approach (adapted from Kurama et al.[18]).

Structure demands — Structure demands quantify roof displacement, story drift, and base shear demands for the two seismic demand levels identified above. For buildings with unbonded post-tensioned precast concrete walls as the primary lateral load resisting system, the structure base shear demands are established in terms of the wall base shear demands. For the design level ground motion, the demands include the wall design base shear demand, V_d, the wall maximum roof displacement demand, Δ_d, and the maximum story drift demand, δ_d. For the maximum considered ground motion, the demands are the maximum roof displacement demand, Δ_s, and the maximum wall base shear demand, V_{max}. Estimation of the structure demands is described later.

Design Objectives

Performance-based design requires design objectives to relate the expected performance levels to the seismic demand levels described above. The proposed design approach for buildings with unbonded post-tensioned precast walls has two objectives: (1) to not exceed the immediate occupancy performance level under the design level ground motion, and (2) to not exceed the collapse prevention performance level under the maximum considered ground motion. These objectives are illustrated in Fig. 8.

The required performance of an unbonded post-tensioned precast concrete wall under the design level ground motion is as follows (see Fig. 7): (1) the wall responds in a nonlinear-elastic manner, with the nonlinear response primarily due to gap opening along the horizontal joints, and partially from nonlinear behavior of the panel concrete in compression; (2) the vertical joint connectors yield in shear; (3) the post-tensioning steel remains linear-elastic; (4) the wall panels remain nearly linear-elastic with minimal cracking, but with spalling of cover concrete near the base at the compression edge of the panels; (5) due to post-tensioning, the wall has a self-centering capability resulting in minimal residual post-ground-motion lateral displacements; (6) shear slip of the panels along the panel-to-foundation connections does not occur; and (7) the resistance of the wall to gravity and lateral loads does not deteriorate. Since the immediate occupancy performance level is reached when yielding of the post-tensioning steel occurs (at Δ_{llp}), the first objective is achieved if Δ_{llp} is not exceeded under the design level ground motion (Fig. 8).

The required performance of an unbonded post-tensioned precast concrete wall under the maximum considered ground motion is as follows (see Fig. 7): (1) axial-flexural compression failure in the wall panels does not occur; (2) the post-tensioning steel yields, but the nonlinear strains in the steel are small because the steel is unbonded; (3) some loss of prestress occurs upon load reversal as a result of inelastic straining in the post-tensioning steel; (4) upon reloading, the lateral stiffness of the wall deteriorates due to the loss of prestress, but the base shear capacity is maintained because the force in the post-tensioning steel on the tension side of the panels (despite having lost some prestress) will still reach its yield force; (5) due to the remaining prestress forces, the wall has a self-centering capability resulting in minimal residual post-ground-motion lateral displacements; and (6) shear slip along the panel-to-foundation connections does not occur.

Since the collapse prevention performance level is reached when axial-flexural compression failure of the wall (crushing of the confined concrete) occurs (at Δ_{ccc}), the second objective is achieved if Δ_{ccc} is not exceeded under the

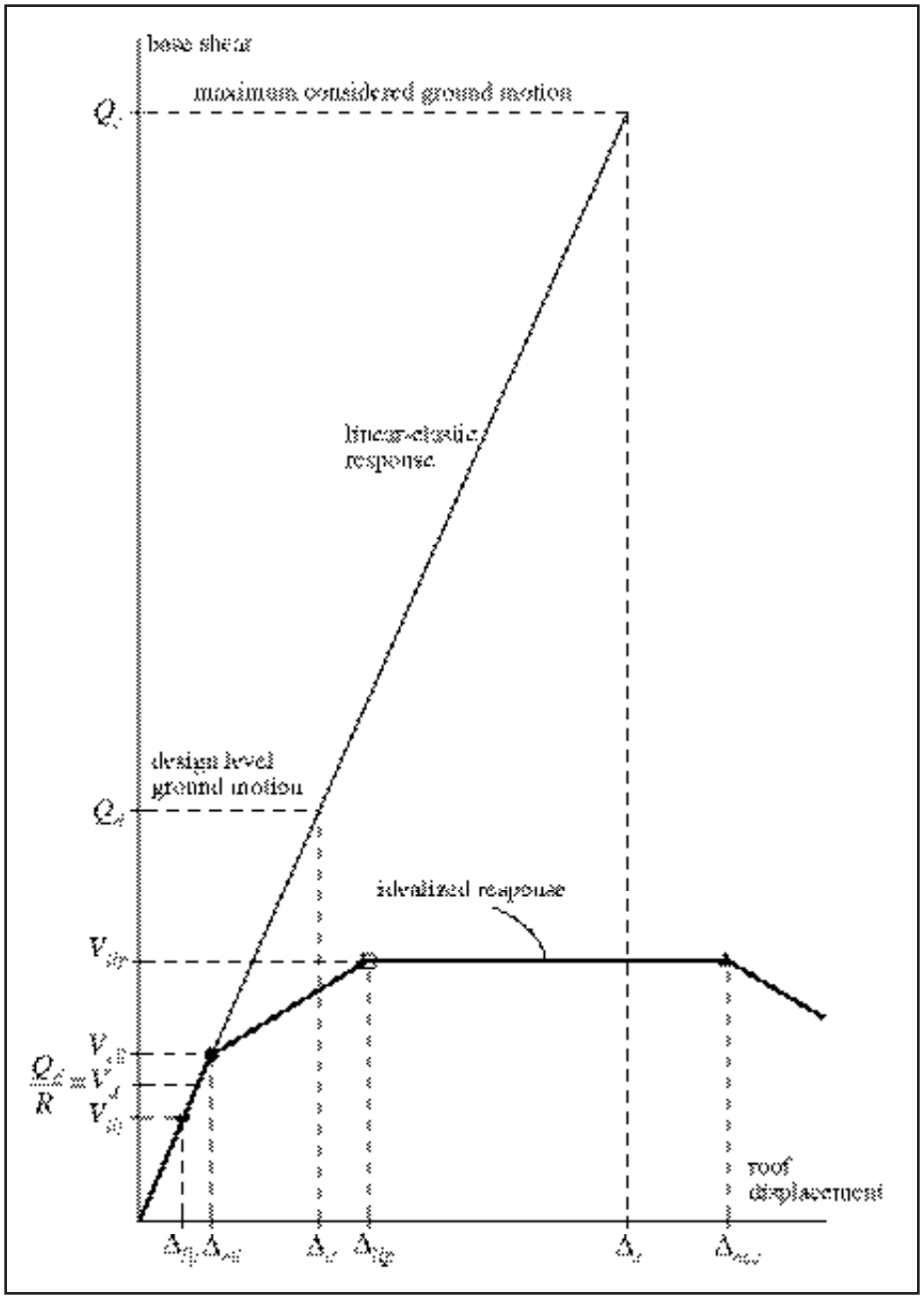

Fig. 9. Design criteria to control axial-flexural behavior (adapted from Kurama et al.[18]).

maximum considered ground motion (Fig. 8). Performance-based design requires seismic design criteria to compare structure capacities with structure demands. The design objectives are achieved if the structure capacities exceed the structure demands.

Seismic Design Criteria

Design criteria described here are used to control the axial-flexural behavior of unbonded post-tensioned precast walls with vertical joint connectors. The estimation of design capacities and of design demands is covered in subsequent sections.

Criterion 1, softening — This design criterion, which controls softening of an unbonded post-tensioned precast wall under lateral load, prevents a premature reduction in the lateral stiffness of the wall. Accordingly, the base shear corresponding to the effective linear limit state, V_{ell}, should not be less than the base shear at which softening is acceptable, which can be related to the wall design base shear demand, V_d. A factor α_d is applied to V_d to define the base shear at which softening of a wall is allowed to occur. Thus:

$$V_{ell} \geq \alpha_d V_d = \alpha_d \frac{Q_d}{R} \qquad (16)$$

In this paper, V_d is determined using the equivalent lateral force procedure in the NEHRP recommended provisions[14] and is equal to the linear-elastic base shear demand for the design level ground motion, Q_d divided by a response modification coefficient, R, equal to 5 in accordance with NEHRP[14] (Fig. 9). A minimum value of 0.65 is recommended for α_d. Dynamic analysis results from Kurama et al.[20] show that a wall designed to soften this early (i.e., $V_{ell} = 0.65V_d$) will not undergo significantly increased drift demands compared to a wall that softens at V_d (i.e., $V_{ell} = 1.0V_d$). In the present study, $\alpha_d = 1.0$ is used.

Criterion 2, base moment capacity — This design criterion controls the base moment capacity (as governed by axial-flexural behavior) of the wall. The structure demands specified in building codes[14-16] are quantified in terms of base shear under equivalent lateral forces. Thus, the base moment capacity of the wall is expressed in terms of the base shear capacity of the wall (as governed by axial-flexural behavior). The base shear capacity of an unbonded post-tensioned precast concrete wall corresponds to the base shear at yielding of the post-tensioning steel (V_{llp}), as shown in Fig. 7. According to this design criterion, V_{llp} should not be less than the wall design base shear demand, V_d. A capacity reduction factor, Φ_f, is applied to V_{llp}. Accordingly:

$$\Phi_f V_{llp} \geq V_d = \frac{Q_d}{R} \qquad (17)$$

If unbonded post-tensioned walls are treated as reinforced members subjected to axial compression with flexure, a

value of 0.7 is required for Φ_f in accordance with the ACI 318 Code.[21] Properly designed unbonded post-tensioned walls, however, are essentially flexural members, with substantial ductility. Flexural capacity can be accurately predicted,[13] and therefore a value of 0.9 may be appropriate for Φ_f. In the present study, a value of 0.75 is used for Φ_f.

Criterion 3, yielding of post-tensioning steel — According to this design criterion, which controls yielding of the post-tensioning steel, the roof displacement corresponding to yielding of the post-tensioning steel, Δ_{llp}, should not be less than the roof displacement demand for the design level ground motion, Δ_d (see Fig. 9). That is:

$$\Delta_{llp} \geq \Delta_d \qquad (18)$$

Criterion 4, gap closure at the base — This design criterion controls the initial prestress force on the two groups of post-tensioning steel in the panels, T_{1i} and T_{2i}, to ensure that the gap opening, which develops at the base of the panels due to lateral loads, closes after the removal of the lateral loads. Fig. 10 shows five displacement states that can develop as gap opening behavior occurs at the base of a rigid interior panel under the action of lateral loads, an eccentric gravity force, and unequal initial prestress forces on the groups of post-tensioning steel: (1) undisplaced position with full contact at the base of the panel; (2) gap opening with contact at the right edge of the panel, yielding of the vertical joint connectors, and yielding of the left post-tensioning steel group; (3) undisplaced position with full contact at the base of the panel, and a reduction in prestress of the left post-tensioning steel group where Φ_{gc} is the initial prestress reduction factor, which is selected by the designer (note that Φ_{gc} = 0.75 is used in the present study); (4) gap opening with contact at the left edge of the panel, and yielding of the right post-tensioning steel group; (5) undisplaced position with full contact at the base of the panel (provided T_{1i} and T_{2i} are large enough), and a reduction in prestress of the right post-tensioning steel group.

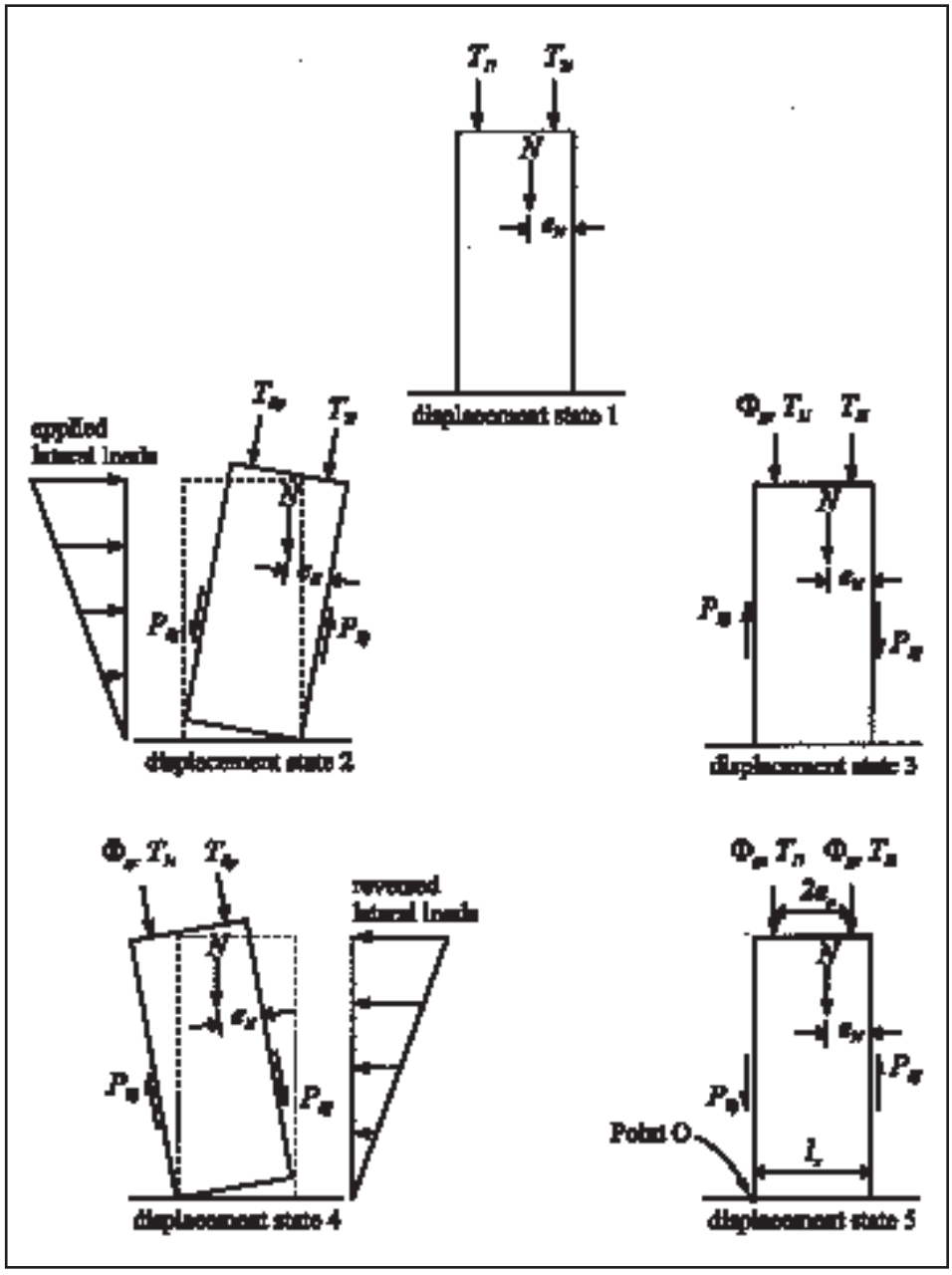

Fig. 10. Five displacement states of a rocking panel.

Summing moments about Point O in Displacement State 5 of Fig. 10 gives the following expression:

$$\Phi_{gc}\left[T_{1i}\left(\frac{l_x}{2}-e_p\right)+T_{2i}\left(\frac{l_x}{2}+e_p\right)\right]+N\left(l_x-e_N\right)\geq P_{llj}l_x \qquad (19)$$

where l_x is the length of the panel, N is the gravity load on a panel, e_N is the eccentricity of the gravity load N measured from the right edge of the panel, and P_{llj} is the total shear force in the vertical joint connectors at yield. The left terms in Eq. (19) represent the moments that force the gap to close after the removal of lateral loads, whereas the term on the right side of the equation represents the moment that causes the gap at the base to remain open. If Eq. (19) is satisfied, the gap will close at the panel-foundation joint. Eq. (19) is derived for a panel that is subjected to cyclic lateral loads, where the lateral loads are first applied to the right, causing Displacement State 2 in Fig. 10, and are then reversed, causing Displacement State 4

in Fig. 10. If the lateral loads are first applied to the left, Eq. (19) is valid as long as T_{1i} and T_{2i} are interchanged and e_N is measured from the *left* edge of the panel.

Criterion 5, story drift — This design criterion controls the maximum story drift under the design level ground motion to control the lateral stiffness of the walls and to control damage to basic access and life safety systems. According to this design criterion, the estimated maximum story drift demand for the design level ground motion, δ_d, should not exceed the allowable story drift, δ_{all} (which in the present study equals 2 percent based on the NEHRP[14] recommended provisions). Thus:

$$\delta_{all} \geq \delta_d \tag{20}$$

Criterion 6, crushing of confined concrete — According to this design criterion, which controls the axial-flexural compression failure of the walls, the roof displacement capacity corresponding to crushing of confined concrete, Δ_{ccc}, should not be less than the roof displacement demand for the maximum considered ground motion, Δ_s. Thus:

$$\Delta_{ccc} \geq \Delta_s \tag{21}$$

Criterion 7, fracture of post-tensioning steel — According to this design criterion, which ensures that fracture of the post-tensioning steel does not occur, the roof displacement corresponding to fracture of the post-tensioning steel, Δ_{fp}, should be greater than the roof displacement corresponding to crushing of confined concrete, Δ_{ccc}. Thus:

$$\Delta_{fp} > \Delta_{ccc} \tag{22}$$

Other criteria — A criterion is needed to control the length and height of the confined concrete region near the base of the panels (Fig. 1). This criterion was developed by Kurama et al.[18] for unbonded post-tensioned walls with horizontal joints, but is not considered in the present study. Another criterion is required to prevent shear slip along the panel-to-foundation connections under the action of earthquake loads. This criterion (developed by Kurama et al.[18]) compares estimated maximum wall shear demands with the shear friction capacity of the wall-foundation joint. Finally, a criterion is needed to prevent a premature failure of the gravity load resisting system of the building, which is separate from the lateral load resisting system, due to an excessive lateral displacement of the structure. This criterion (developed by Kurama et al.[18]) states that the roof displacement demand for the maximum considered ground motion, Δ_s, should not exceed the roof displacement of the structure corresponding to failure of the gravity load resisting system, Δ_g. As noted earlier, it is assumed that the gravity load resisting system can sustain a roof drift of 2.5 percent without failure. Accordingly, Δ_s should not exceed $0.025H_w$.

Estimation of Structure Design Capacities

The previous section described the design criteria that are used to control the behavior of a wall. This section describes how the structure capacity for each design criterion is calculated.

Criterion 1 capacity (V_{ell}) — The base shear corresponding to the effective linear limit state, V_{ell}, of an unbonded post-tensioned precast concrete wall with vertical joint connectors is calculated using Eq. (4). Eq. (4) applies to a wall with numerous panels and floor levels and eccentric gravity forces. For the specific case of the prototype wall considered in the design example, V_{ell} is calculated using Eq. (6).

Criterion 2 capacity (V_{llp}) — The base shear capacity, V_{llp}, of an unbonded post-tensioned precast wall with vertical joint connectors is computed from Eq. (11). Eq. (11) applies to a wall with numerous panels and floor levels and eccentric gravity forces. For the specific case of the prototype wall considered in the design example, V_{llp} is calculated using Eq. (13).

Criterion 3 capacity (Δ_{llp}) — The roof displacement corresponding to yielding of the post-tensioning steel, Δ_{llp}, of an unbonded post-tensioned precast concrete wall with vertical joint connectors is calculated using Eq. (14).

Criterion 4 capacity (gap closure) — The moments that force gap closure at the base of the wall after the lateral loads are removed are computed by the terms on the left side of Eq. (19).

Criterion 5 capacity (δ_{all}) — The maximum allowable story drift for the design level ground motion, δ_{all}, is equal to 2.0 percent based on the NEHRP recommended provisions.[14] This value is applicable to buildings assigned to Seismic Use Group I in the NEHRP recommended provisions.[14]

Criterion 6 capacity (Δ_{ccc}) — A closed form expression has not been derived to estimate the roof displacement capacity corresponding to crushing of confined concrete (Δ_{ccc}). However, Δ_{ccc} can be determined by performing a nonlinear static push-over analysis of a fiber-based model of the wall using the DRAIN-2DX program[22] under a building code-specified distribution of equivalent lateral forces. The fiber-based model of an unbonded post-tensioned precast wall with vertical joints and ductile connectors is discussed by the authors in an accompanying paper.[1]

Criterion 7 capacity (Δ_{fp}) — A closed form expression has not been derived to estimate the roof displacement capacity corresponding to fracture of the post-tensioning steel (Δ_{fp}). However, Δ_{fp} can be determined by performing a nonlinear static push-over analysis of a fiber-based model of the wall using the DRAIN-2DX program[22] under a building code-specified distribution of equivalent lateral forces. The fiber-based model of an unbonded post-tensioned precast concrete wall with vertical joints and ductile connectors is discussed by the authors in the companion paper.[1]

Estimation of Structure Design Demands

This section describes the estimation of design demands for each design criterion of the proposed seismic design approach discussed earlier. The following treats buildings with no *plan* or *vertical* structural irregularities.

Criteria 1 and 2 demands (V_d) — The wall design base shear demand for the design level ground motion, V_d, is estimated by distributing the building code-specified structure

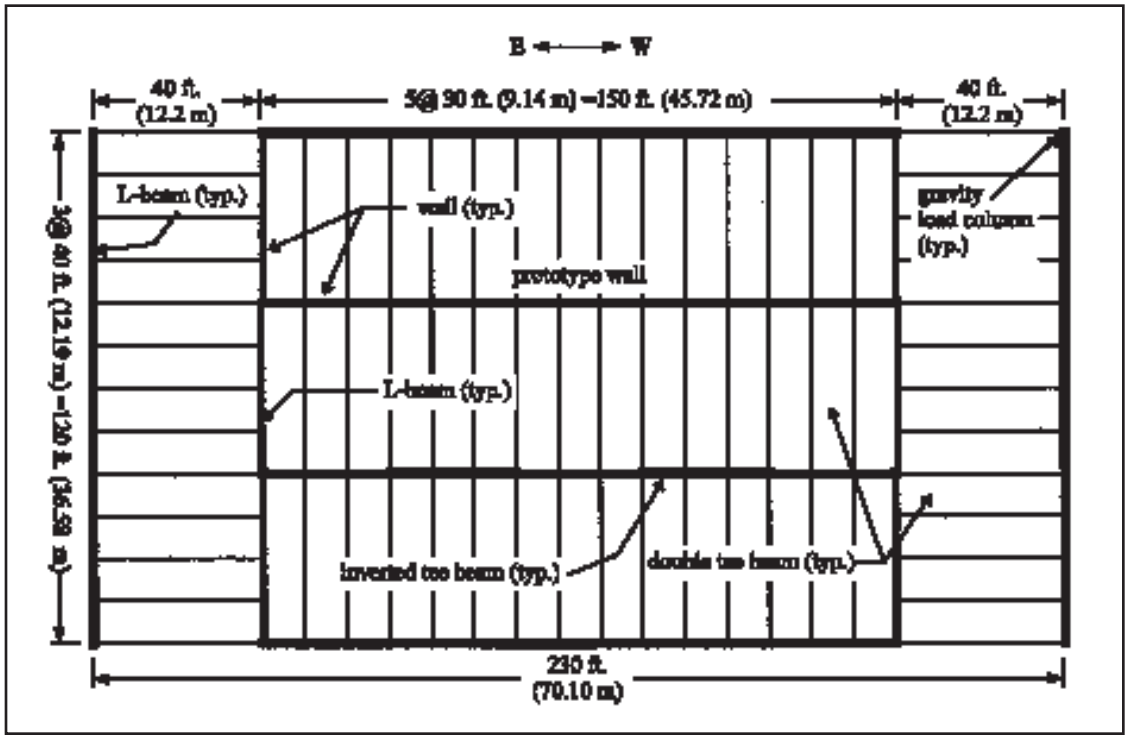

Fig. 11. Plan view of the prototype structure.

design base shear demand, V_d^s, between the unbonded post-tensioned precast concrete walls and other lateral load resisting members in a structure. The structure design base shear demand depends on the properties of the structure, the seismicity of the region where the building is located, and the soil profile at the building site, and is given by:

$$V_d^s = WC_s \tag{23}$$

where W is the seismic weight of the structure, which is composed of the building self-weight and dead load only (live load is excluded). Partition loads of 20 psf (98 kg/m^2), which are part of the live loads used in the design of a building as per UBC,[15] are included in the seismic weight computation. C_s is the seismic response coefficient defined in various building codes. The NEHRP[14] definition of C_s is adopted in this study.

Criterion 3 demand (Δ_d) — The maximum wall roof displacement demand for the design level ground motion, Δ_d, is assumed to be equal to the linear-elastic roof displacement demand under this ground motion. The linear-elastic roof displacement demand is estimated by dividing the wall linear-elastic base shear demand for the design level ground motion, Q_d, by the wall initial lateral stiffness (Fig. 9). This estimation is based on the so-called equal displacement assumption. Other displacement coefficient methods could be used.[23-25] The wall initial lateral stiffness can be approximated as $k_{wi} = V_{ell}/\Delta_{ell}$, where V_{ell} is calculated using Eq. (4) [Eq. (6) for the prototype wall] and Δ_{ell} is calculated using Eq. (7) [Eq. (10) for the prototype wall]. Therefore:

$$\Delta_d = Q_d \frac{\Delta_{ell}}{V_{ell}} \tag{24}$$

where

$$Q_d = V_d R$$

R is the response modification coefficient, which is equal to 5 for special reinforced concrete shear walls in the NEHRP provisions.[14]

Criterion 4 demand (gap closure) — The demand for gap closure at the base of the wall panels in accordance with Criterion 4 is given by the term on the right side of Eq. (19).

Criterion 5 demand (δ_d) — The maximum story drift demand for the design level ground motion, δ_d, is determined by:

$$\delta_d(\%) = \frac{C_d \delta_{je}}{Ih} = \frac{C_d\left(\Delta_j - \Delta_{j-1}\right)}{Ih} \tag{25}$$

where h is the story height, C_d is the deflection amplification factor (equal to 5 when the NEHRP recommended provisions[14] are used), and I is the occupancy importance factor assigned to the structure (as given in the NEHRP recommended provisions[14]). δ_{je} is the linear elastic story drift, defined as the difference between the lateral deflections of the floor level above and below the story under consideration ($\Delta_j - \Delta_{j-1}$), and is computed for each story by an elastic analysis of the wall under a code-specified distribution of equivalent lateral forces. The elastic lateral deflection at an arbitrary floor level j of a wall with r stories, n panels of the same geometry, eccentric gravity forces on each panel that can vary along the height of the wall, and lateral loads applied at each floor level, can be computed by:

$$\Delta_j = \Delta_{Fj} + \Delta_{Sj} + \Delta_{Nj} + \Delta_{Pj} \tag{26}$$

Table 1. Summary of key design parameters.

Wall parameters	Number of panels, n	3
	Panel length, l_x	108 in.
	Wall length, $l_w = nl_x$	324 in.
	Height, H_w	336 in.
	Thickness, t_w	12 in.
	Stories, r	2
	Floor 1 height ratio, r_{H1}	0.5
	Roof height ratio, r_{Hr}	1.0
	I_w	3.828×10^6 in.^{4}
	A'_w	3.24×10^3 sq in.
Vertical joint parameter	P_{llj}	162 kips
Prestress parameters	A_p	4.0 sq in.
	e_p	27 in.
	E_p	29,000 ksi
	f_{pl}	128 ksi
	f_{pu}	160 ksi
	$f_{pi} = 0.60f_{pu}$	96 ksi
	P_i	384 kips
	T_{1i}	192 kips
	T_{2i}	192 kips
	$T_{llp} = f_{pl}A_p/2$	256 kips
	Φ_{gc} (assumed)	0.75
Concrete properties	f'_c	6000 psi
	E_c	4415 ksi
	G_c	1920 ksi
	ρ_{sp}	7.5 percent
Load parameters	N	82.7 kips
	$e_{N1} = e_{N2} = e_{N3} = l_x/2$	54 in.
	Floor 1 load ratio, r_{F1}*	0.44
	Roof load ratio, r_{Fr}*	0.56

Note: 1 in. = 25.4 mm; 1 sq in. = 645 mm^2; 1 kip = 4.45 kN; 1 ksi = 6.895 MPa.
*Obtained from a code-specified distribution of equivalent lateral forces.

where

$$\Delta_{Fj} = \sum_{i=1,j} \frac{1}{2E_cI_w}(r_{Fi}V_d)r_{Hi}^2H_w^3\left(r_{Hj} - \frac{1}{3}r_{Hi}\right) + \sum_{i=j+1,r} \frac{1}{2E_cI_w}(r_{Fi}V_d)r_{Hj}^2H_w^3\left(r_{Hi} - \frac{1}{3}r_{Hj}\right)$$

$$\Delta_{Sj} = \sum_{i=1,j} \frac{r_{Fi}V_dr_{Hi}H_w}{G_cA'_w} + \sum_{i=j+1,r} \frac{r_{Fi}V_dr_{Hj}H_w}{G_cA'_w}$$

$$\Delta_{Nj} = \sum_{i=1,j} \frac{1}{E_cI_w}M_{w,i}(r_{Hi}H_w)H_w\left(r_{Hj} - \frac{1}{2}r_{Hi}\right) + \sum_{i=j+1,r} \frac{1}{2E_cI_w}M_{w,i}(r_{Hj}H_w)^2$$

$$\Delta_{Pj} = \frac{ne_p(T_2 - T_1)(r_{Hj}H_w)^2}{2E_cI_w}$$

$$T_1 = T_{1i}$$

$$T_2 = T_{2i}$$

Eq. (26) is derived for the wall shown in Fig. 3 in the same manner that Eq. (7) was derived for the roof displacement corresponding to the effective linear limit state. Δ_{Fj} is the elastic deflection of the wall at floor j in flexure due to lateral loads. Δ_{Fj} is obtained using the principle of superposition. The first summation term in the Δ_{Fj} equation represents the total lateral deflection of floor j caused by lateral loads applied at floor j and at all the floor levels below it. The second summation term in the Δ_{Fj} equation represents the total lateral deflection of floor j caused by lateral loads applied at the floor levels above floor j.

The deflection of the wall at floor j due to elastic shear deformations, obtained using the principle of superposition, is denoted as Δ_{Sj}. Δ_{Nj} is the elastic deflection of the wall at floor j in flexure due to eccentrically applied gravity forces. The notation $M_{w,i}$ in the Δ_{Nj} equation represents a concentrated wall moment (measured positive in the clockwise direction) applied at floor level i which is calculated using Eq. (8). Δ_{Pj} is the elastic deflection of the wall at floor j caused by the application of different initial prestress forces in the left post-tensioning steel group and the right post-tensioning steel group of each panel, denoted by T_{1i} and T_{2i}, respectively. The initial prestress forces, T_{1i} and T_{2i}, are the same for all the panels. The moment produced by the unbalanced prestress forces on a panel is added over the panels and is applied to the wall as a concentrated moment (measured positive in the clockwise direction) at the roof level, because the post-tensioning steel is unbonded over the entire height of the wall, and thus the wall is subjected to a constant moment over its entire height.

Eq. (26) is derived for a wall that has lateral loads applied to the right, as shown in Fig. 3. If the lateral loads are applied to the left, Eq. (26) is valid as long as T_1 and T_2 are interchanged, e_N is measured from the *left* edge of the panels, $M_{w,i}$ is measured positive in the *counter-clockwise* direction, and the concentrated wall moment produced by unbalanced prestress forces on the panels is measured positive in the *counter-clockwise* direction.

To determine δ_d for the prototype wall considered in the design example, composed of two stories, three panels with the same geometry, the same gravity forces N acting at the center of each panel, and the forces T_1 and T_2 each equal to half the total initial prestress force on a panel, the elastic deflection of the roof Δ_r and of the first floor Δ_1 are required. These are computed as:

$$\Delta_r = \Delta_{Fr} + \Delta_{Sr} \tag{27}$$

and

$$\Delta_1 = \Delta_{F1} + \Delta_{S1} \tag{28}$$

where

$$\Delta_{Fr} = \frac{1}{2E_cI_w}\left[(r_{F1}V_d)r_{H1}{}^2H_w{}^3\left(r_{Hr} - \frac{1}{3}r_{H1}\right) + (r_{Fr}V_d)r_{Hr}{}^2H_w{}^3\left(r_{Hr} - \frac{1}{3}r_{Hr}\right)\right]$$

$$\Delta_{Sr} = \frac{1}{G_cA'_w}(r_{F1}V_dr_{H1}H_w + r_{Fr}V_dr_{Hr}H_w)$$

$$\Delta_{F1} = \frac{1}{2E_c I_w}\left[(r_{F1}V_d)r_{H1}^{\,2}H_w^{\,3}\left(r_{H1}-\frac{1}{3}r_{H1}\right)+(r_{Fr}V_d)r_{H1}^{\,2}H_w^{\,3}\left(r_{Hr}-\frac{1}{3}r_{H1}\right)\right]$$

$$\Delta_{S1} = \frac{1}{G_c A'_w}\left(r_{F1}V_d r_{H1}H_w + r_{Fr}V_d r_{H1}H_w\right)$$

Δ_{Fr} and Δ_{F1} are the elastic deflections of the roof and the first floor level, respectively, in flexure due to lateral forces. Δ_{Sr} and Δ_{S1} are the deflections of the roof and the first floor level, respectively, due to elastic shear deformations of the prototype wall. The elastic story drift of the first story, δ_{1e}, equals $\Delta_{F1} + \Delta_{S1}$, and the elastic story drift of the second story, δ_{2e}, equals $(\Delta_{F2} + \Delta_{S2}) - (\Delta_{F1} + \Delta_{S1})$, where Δ_{F2} and Δ_{S2} are equal to Δ_{Fr} and Δ_{Sr}, respectively, for the prototype wall.

Criterion 6 demand (Δ_s) — The maximum wall roof displacement demand for the maximum considered ground motion, Δ_s, is computed as:

$$\Delta_s = \alpha_s \Delta_d \qquad (29)$$

As noted earlier, the NEHRP recommended provisions[14] define the design level ground motion as having a ground shaking intensity that is two-thirds of the maximum considered earthquake ground motion. Therefore, $\Delta_d = 2\Delta_s/3$, or $\Delta_s = 1.5\Delta_d$. According to the NEHRP recommended provisions,[14] the factor of 1.5 is a lower bound estimate of the margin against collapse of a structure. Therefore, α_s should not be less than 1.5. In the present study, a conservative value of 2.5 is used for α_s. Δ_d in Eq. (29) is computed using Eq. (24).

Criterion 7 demand (Δ_{ccc}) — See Criterion 6 capacity.

DESIGN EXAMPLE

The objective is to design a prototype wall using the proposed design approach presented earlier. The example concentrates on the seismic design of a wall for the two-story prototype structure shown in Fig. 11 under a ground motion in the E-W direction. Table 1 summarizes various key parameters used in the design of the wall. These include the wall, vertical joint, prestress, and load parameters, as well as concrete material properties. The following steps are recommended for applying the proposed design approach:

1. Select initial wall, vertical joint, and prestress parameters (see Table 1). These parameters describe the prototype wall, which is two stories tall and is composed of three panels that have the same geometry.

2. Define the load parameters (see Table 1). The magnitude of the gravity force on each panel, N_k (k = 1 to n), and its location on each panel, e_{Nk} (k = 1 to n), depend on the building layout and the number of panels in a wall (n). For the prototype wall, which has three panels, the gravity forces are assumed to act at the center of each panel. Thus, $e_{N1} = e_{N2} = e_{N3} = l_x/2$ (see Table 1).

3. Define the concrete properties (see Table 1). The prototype wall uses interlocking spirals to confine the concrete at the ends of each panel throughout the height of the first story. The level of confinement provided by the spirals is quantified in terms of a volumetric ratio of spiral reinforcement, ρ_{sp}. This parameter controls the capacity for Criterion 6 of the design approach.

4. Calculate the structure seismic properties and demands in accordance with the applicable building code (the NEHRP recommended provisions[14] are used in this example). Table 2 summarizes the seismic properties and demands computed for the prototype structure.

5. Calculate the wall design base shear demand, V_d, using Eq. (16). For the prototype wall, V_d = 348 kips (1549 kN) in accordance with the NEHRP recommended provisions.[14]

6. Estimate and compare the wall seismic capacities and demands for each criterion of the proposed design approach. Table 3 summarizes the design criteria and shows the estimated seismic capacities and demands for the prototype wall.

Table 3 shows that the prototype wall satisfies the seismic design criteria of the proposed design approach. If a criterion of the design approach is not satisfied, certain parameters can be changed to ensure that the criterion is satisfied.

Table 2. Estimated seismic properties and demands for the prototype structure.

W (kips)	T (seconds)	V_d^s (kips)	Q_d^s (kips)
7289	0.24	1604	7218

Note: 1 kip = 4.45 kN.

Table 3. Estimated seismic capacities and demands for the prototype wall.

	Seismic design criteria	Capacity	Demand
Criterion 1	$V_{ell} \geq \alpha_d V_d = \alpha_d Q_d / R$ $(0.65 \leq \alpha_d \leq 1.0)$ (Eq. 16)	V_{ell} = 372 kips (Eq. 6)	α_d = 1.0 V_d = 348 kips
Criterion 2	$\Phi_f V_{llp} \geq V_d$ $(0.7 \leq \Phi_f \leq 0.9)$ (Eq. 17)	Φ_f = 0.75 V_{llp} = 460 (Eq. 13)	V_d = 348 kips
Criterion 3	$\Delta_{llp} \geq \Delta_d$ (Eq. 18)	Δ_{llp} = 1.8 in. (Eq. 14)	Δ_d = 0.98 in. (Eq. 24)
Criterion 4	$\Phi_{gc}[T_{1i}(l_x/2 - e_p) + T_{2i}(l_x/2 + e_p)] + N(l_x - e_N) \geq P_{llj} l_x$ (Eq. 19)	20,000 kip-ft (Eq. 19)	18,000 kip-ft (Eq. 19)
Criterion 5	$\delta_{all} \geq \delta_d$ (Eq. 20)	δ_{all} = 2.0 percent (NEHRP[14])	δ_d = 0.4 percent (Eq. 25)
Criterion 6	$\Delta_{ccc} \geq \Delta_s$ (Eq. 21)	Δ_{ccc} > 6.7 in.* (> 2 percent roof drift)	Δ_s = 2.2 in. (Eq. 29)
Criterion 7	$\Delta_{fp} > \Delta_{ccc}$	Δ_{fp} > 6.7 in.* (> 2 percent roof drift)	Δ_{ccc} > 6.7 in.* (> 2 percent roof drift)

Note: 1 in. = 25.4 mm; 1 kip = 4.45 kN; 1 kip-ft = 1.36 kN-m.
* Closed-form expression not developed. Result obtained from a nonlinear static push-over analysis.[1]

These recommendations are provided in the companion paper[1] which studies the influence of certain parameters on the behavior (capacities) of an unbonded post-tensioned precast wall with vertical joint connectors.

CONCLUSIONS

This research investigates the seismic design of walls composed of precast concrete panels that are attached to each other along vertical joints with ductile connectors, and to the foundation along horizontal joints with post-tensioning steel that is not bonded to the concrete. Closed-form expressions are derived to estimate key values that define the lateral load behavior of the walls. A seismic design approach for the walls is proposed using the base shear demands recommended by current model building codes.

A prototype wall is designed to satisfy the seismic design criteria of the proposed design approach. In particular, the prototype wall satisfies nonlinear displacement demands under code-specified design level ground motions without yielding in the post-tensioning steel, but with yielding and energy dissipation in the vertical joint connectors. The prototype wall also satisfies nonlinear displacement demands under maximum considered ground motions without fracture of the post-tensioning steel, or compression failure of the concrete in the wall panels. Study results demonstrate that unbonded post-tensioned precast walls with vertical joint connectors are well suited for use as seismic resistance of building structures.

A companion paper[1] presents results from an analytical parameter study of unbonded post-tensioned walls with ductile vertical joint connectors. The analytical study verifies the accuracy of the closed-form expressions presented in this paper and discusses the influence of certain wall parameters on the lateral load response of the walls. Based on the analytical results, recommendations are provided to ensure that the seismic design criteria presented in this paper are satisfied.

ACKNOWLEDGMENT

This research was funded by the Precast/Prestressed Concrete Institute (PCI) and by the Center for Advanced Technology for Large Structural Systems (ATLSS) at Lehigh University in Bethlehem, Pennsylvania. The support from the sponsors is gratefully acknowledged. Findings and conclusions presented in this paper are those of the authors and do not necessarily reflect the views of the sponsors. The authors are grateful to the PCI JOURNAL reviewers for their thoughtful and constructive comments.

REFERENCES

1. Perez, F. J., Pessiki, S., and Sause, R., "Lateral Load Behavior of Unbonded Post-Tensioned Precast Concrete Walls with Vertical Joints," scheduled for publication in the March-April 2004 PCI JOURNAL.
2. Fintel, M., "Performance of Buildings with Shear Walls in Earthquakes of the Last Thirty Years," PCI JOURNAL, V. 40, No. 3, May-June 1995, pp. 62-80.
3. Kurama, Y., Sause, R., Pessiki, S., and Lu, L.-W., "Lateral Load Behavior and Seismic Design of Unbonded Post-Tensioned Precast Concrete Walls," *ACI Structural Journal*, V. 96, No. 4, July-August 1999, pp. 622-632.
4. Shultz, A. E., and Magaña, R. A., "Seismic Behavior of Connections in Precast Concrete Walls," Mete A. Sozen Symposium, SP-162, American Concrete Institute, Farmington Hills, MI, 1996.
5. Nakaki, S. D., Stanton, J. F., and Sritharan, S., "An Overview of the PRESSS Five-Story Precast Test Building," PCI JOURNAL, V. 44, No. 2, March-April 1999, pp. 26-39.
6. Priestley, M. J. N., Sritharan, S., Conley, J. R., and Pampanin, S., "Preliminary Results and Conclusions From the PRESSS Five-Story Precast Concrete Test Building," PCI JOURNAL, V. 44, No. 6, November-December 1999, pp. 42-67.
7. Stanton, J. F., and Nakaki, S. D., "Design Guidelines for Precast Concrete Seismic Structural Systems," PREcast Seismic Structural Systems (PRESSS) Report No. 01/03-09, University of Washington (UW) Report No. SM 02-02, Department of Civil Engineering, University of Washington, Seattle, WA, February 2002.
8. Perez, F. J., "Lateral Load Behavior and Design of Unbonded Post-Tensioned Precast Concrete Walls with Ductile Vertical Joint Connectors," M.S. Thesis, Department of Civil and Environmental Engineering, Lehigh University, Bethlehem, PA, December 1998, 201 pp.
9. Perez, F. J., Pessiki, S., and Sause, R., "Lateral Load Behavior and Design of Unbonded Post-Tensioned Precast Concrete Walls with Ductile Vertical Joint Connectors," Center for Advanced Technology for Large Structural Systems (ATLSS) Report No. 99-01, Lehigh University, Bethlehem, PA, January 1999, 127 pp.
10. Priestley, M. J. N., and Tao, J. R., "Seismic Response of Precast Prestressed Concrete Frames with Partially Debonded Tendons," PCI JOURNAL, V. 38, No. 1, January-February 1993, pp. 58-69.
11. Mander, J., Priestley, M., and Park, R., "Theoretical Stress-Strain Model for Confined Concrete," *Journal of Structural Engineering*, V. 114, No. 8, August 1988, pp. 1804-1826.
12. Mander, J., Priestley, M., and Park, R., "Observed Stress-Strain Behavior of Confined Concrete," *Journal of Structural Engineering*, V. 114, No. 8, August 1988, pp. 1827-1849.
13. Perez, F. J., Pessiki, S., Sause, R., and Lu, L.-W., "Lateral Load Tests of Unbonded Post-Tensioned Precast Concrete Walls," SP-211-8, American Concrete Institute, Farmington Hills, MI, 2003, pp. 161-182.
14. BSSC, "NEHRP Recommended Provisions for the Development of Seismic Regulations for New Buildings," Building Seismic Safety Council, Washington, DC, 1997.
15. ICBO, *Uniform Building Code*, International Conference of Building Officials, Whittier, CA, 1997.
16. ICC, "International Building Code 2000," International Code Council, Falls Church, VA, 2001.
17. BSSC, "NEHRP Guidelines for the Seismic Rehabilitation of Buildings," FEMA-273, Building Seismic Safety Council, Washington, DC, 1997.
18. Kurama, Y., Pessiki, S., Sause, R., and Lu, L.-W., "Seismic Behavior and Design of Unbonded Post-Tensioned Precast Concrete Walls," PCI JOURNAL, V. 44, No. 3, May-June 1999, pp. 72-89.
19. Freeman, S., "Racking Tests of High-Rise Building Partitions," *Journal of Structural Engineering*, V. 103, No. ST8, August 1977, pp. 1673-1685.
20. Kurama, Y., Sause, R., Pessiki, S., and Lu, L.-W., "Seismic Response Evaluation of Unbonded Post-Tensioned Precast Walls," *ACI Structural Journal*, V. 99, No. 5, September-October 2002, pp. 641-651.
21. ACI Committee 318, "Building Code Requirements for Structural Concrete (ACI 318-99)," American Concrete Institute, Farmington Hills, MI, 1999.
22. Prakash, V., and Powell, G., "DRAIN-2DX Base Program Description and User Guide; Version 1.10," Report No. UCB/SEMM-93/17, Structural Engineering Mechanics and Materials, Department of Civil Engineering, University of California, Berkeley, CA, November 1993.
23. Miranda, E., "Inelastic Displacement Ratios for Structures on Firm Sites," *Journal of Structural Engineering*, V. 126, No. 10, October 2000, pp. 1150-1159.
24. Ruiz-Garcia, J., and Miranda, E., "Inelastic Displacement Ratios for Evaluation of Existing Structures," *Earthquake Engineering and Structural Dynamics*, V. 32, No. 8, July 2003, pp. 1237-1258.
25. Miranda, E., and Ruiz-Garcia, E., "Evaluation of Approximate Methods to Estimate Maximum Inelastic Displacement Demands," *Earthquake Engineering and Structural Dynamics*, V. 31, No. 3, March 2002, pp. 539-560.

APPENDIX — NOTATION

A_p = total cross-sectional area of post-tensioning steel in a panel
A'_w = effective shear area of wall
C_d = NEHRP deflection amplification factor
C_i = compression stress resultant in concrete after the application of prestress forces and gravity loads
C_k = compression stress resultant at base of panel k
C_{ki} = compression stress resultant on panel k after the application of prestress forces and gravity loads
C_s = NEHRP seismic response coefficient
c_k = length of compression zone at base of panel k
E_c = elastic modulus of concrete
E_p = elastic modulus of post-tensioning steel
e_{Nk} = eccentricity of N_k measured from right edge of panel
e_p = eccentricity of post-tensioning steel from panel centerline to centroid of post-tensioning steel
$F_{k,i}$ = lateral force on panel k at level i
$F_{k,r}$ = lateral force on panel k at roof level
$F_{w,i}$ = lateral force on wall at floor i
$F_{w,r}$ = lateral force on wall at roof level
f'_c = compressive strength of unconfined concrete
f_{pi} = stress in post-tensioning steel after the application of prestress forces and gravity loads (also referred to as the initial stress in the post-tensioning steel)
f_{pl} = yield stress of the post-tensioning steel
f_{pr} = residual stress in post-tensioning steel after unloading from beyond the yield stress
f_{pu} = ultimate strength of post-tensioning steel
G_c = shear modulus of concrete
H_i = height of floor level i measured from the base of the wall
H_r = height of roof level measured from the base of the wall (equal to H_w)
H_w = total wall height
h = story height
I = NEHRP occupancy importance factor assigned to structure
I_w = moment of inertia of the uncracked transformed section of a wall
i = floor level
j = floor level
k = wall panel number
k_{wi} = initial lateral stiffness of wall
l_w = wall length
l_x = panel length
M_{dec} = base moment at the decompression limit state
M_{ell} = base moment at the effective linear limit state due to applied lateral loads
$M_{w,i}$ = moment applied at floor i
N = gravity force on a panel
N_k = gravity force on panel k
n = total number of panels in a wall
P_i = total force in the post-tensioning steel after the application of prestress forces and gravity loads (also referred to as the total initial prestress force on a panel)
P_j = total shear force across a vertical joint
P_{llj} = total shear yield force across a vertical joint
Q_d = wall linear-elastic base shear demand for the design level ground motion
Q_d^s = structure linear-elastic base shear demand for the design level ground motion
Q_s = wall linear-elastic base shear demand for the maximum considered ground motion
Q_s^s = structure linear-elastic base shear demand for the maximum considered ground motion
R = NEHRP response modification coefficient
r = total number of stories in a wall
r_{Fi} = ratio of the force at the ith floor level to the wall base shear
r_{Fr} = ratio of the force at the roof level to the wall base shear
r_{Hi} = ratio of the ith floor height to the total height of the wall
r_{Hr} = ratio of the roof height to the total height of the wall (equal to unity)
T = fundamental period of the structure
T_{llp} = total force in a group of post-tensioning steel at yield
T_1 = total force in a group of post-tensioning steel to the left of panel centerline
T_{1i} = total initial force in a group of post-tensioning steel to the left of panel centerline after the application of prestress forces and gravity loads
T_2 = total force in a group of post-tensioning steel to the right of panel centerline
T_{2i} = total initial force in a group of post-tensioning steel to the right of panel centerline after the application of prestress forces and gravity loads
t_w = wall thickness
V_{ccc} = base shear when confined concrete crushes
V_d = wall design base shear demand
V_d^s = structural design base shear demand
V_{dec} = wall base shear at decompression limit state
V_{ell} = wall base shear at effective linear limit state
V_k = panel base shear
V_{llj} = wall base shear at limit state corresponding to yielding of vertical joint connectors
V_{llp} = wall base shear at limit state corresponding to yielding of post-tensioning steel
V_w = wall base shear
W = structure seismic weight
α_d = factor used to define softening base shear demand
α_s = factor used to define maximum considered roof displacement demand
Δ_{ccc} = roof displacement when confined concrete crushes
Δ_d = roof displacement demand under the design level ground motion
Δ_{dec} = roof displacement at decompression limit state
Δ_{ell} = roof displacement at effective linear limit state
Δ_{Fj} = elastic deflection at floor j due to lateral forces
Δ_{Fr} = elastic wall deflection at roof in flexure due to lateral forces

Δ_{F1} = elastic deflection of first floor in flexure due to lateral forces

Δ_{fp} = roof displacement corresponding to fracture of post-tensioning steel

Δ_g = roof displacement corresponding to failure of the gravity load resisting system

Δ_{go} = roof displacement due to gap opening

Δ_{llj} = roof displacement at limit state corresponding to yielding of vertical joint connectors

Δ_{llp} = roof displacement at limit state corresponding to yielding of post-tensioning steel

Δ_{Nj} = elastic wall deflection at floor j in flexure due to eccentric gravity forces

Δ_{Nr} = elastic wall deflection at roof in flexure due to eccentric gravity force

Δ_{Pj} = elastic wall deflection at floor j due to different initial prestress forces, T_{1i} and T_{2i}

Δ_{Pr} = elastic wall deflection at roof due to different initial prestress forces, T_{1i} and T_{2i}

Δ_r = roof displacement

Δ_s = roof displacement demand for the maximum considered ground motion

Δ_{Sj} = deflection of floor j due to elastic shear deformations

Δ_{Sr} = roof deflection due to elastic shear deformations

Δ_{S1} = deflection of first floor due to elastic shear deformations

Δ_v = gap opening displacement along base of a panel at location of post-tensioning steel centroid on tension side

$\Delta_{v,ell}$ = relative vertical displacement between adjacent panels along the vertical joints at ELL

δ_{all} = allowable story drift

δ_d = maximum story drift demand for the design level ground motion

δ_{je} = linear elastic story drift

ε_{cu} = ultimate compressive strain of confined concrete

ρ_{sp} = volumetric ratio of spiral reinforcement

Φ_f = wall base shear capacity reduction factor

Φ_{gc} = initial prestress reduction factor